THE MOLECULAR BASIS OF AEROBIC METABOLIC REMODELING IN THREESPINE STICKLEBACK IN RESPONSE TO COLD ACCLIMATION

By

Julieanna Inez Orczewska

RECOMMENDED:

Advisory Committee Chair

Chair, Department of Chemistry and Biochemistry

APPROVED:

Dean, College of Natural Science and Mathematics

Dean of the Graduate School

Apr 7, 2011

Date

THE MOLECULAR BASIS OF AEROBIC METABOLIC REMODELING IN THREESPINE STICKLEBACK IN RESPONSE TO COLD ACCLIMATION

A

THESIS

Presented to the Faculty
of the University of Alaska Fairbanks

in Partial Fulfillment of the Requirements
for the Degree of

MASTER OF SCIENCE

By

Julieanna Inez Orczewska, B.A.

Fairbanks, Alaska

May 2011

ABSTRACT

Increases in mitochondrial density during cold acclimation have been documented in many fish species, however the mechanism regulating this process is not understood. The present study sought to characterize metabolic changes in response to cold acclimation and identify how these changes are regulated in oxidative muscle, glycolytic muscle and liver tissue of threespine stickleback, *Gasterosteus aculeatus*. Fish were warm (20°C) or cold (8°C) acclimated for 9 weeks and harvested during acclimation. Mitochondrial volume density was quantified using transmission electron microscopy and aerobic metabolic capacity assessed by measuring the maximal activity of citrate synthase and cytochrome c oxidase. The molecular mechanism mediating changes in aerobic metabolic capacity were assessed by quantifying transcript levels of aerobic metabolic genes and known regulators of mammalian mitochondrial biogenesis using quantitative real-time PCR. Our results indicate that while the maximal activity of aerobic metabolic enzymes increased in all tissues, mitochondrial biogenesis only occurred in oxidative muscle. Our results also suggest that the time course of metabolic remodeling is tissue specific. Lastly, we identified differences in the magnitude and timing of transcriptional and co-transcriptional activators driving metabolic remodeling between each tissue. These results suggest aerobic metabolic remodeling may be triggered by different stimuli in different tissues.

TABLE OF CONTENTS

Page

Page

LIST OF FIGURES

Page

Page

LIST OF TABLES

Page

LIST OF APPENDICES

PREFACE

This thesis represents a culmination of work that was conducted during 2006-2010 at the University of Alaska Fairbanks. This research was undertaken to identify the molecular basis of aerobic metabolic remodeling in response to cold acclimation in fish.

The use of animals was approved by the University of Alaska Fairbanks Institutional Animal Care Committee (135490-2).

Preliminary experiments were designed and obtained by Götz Hartleben in 2006 and the final experiments which are described herein, were performed by Julieanna Orczewska in 2008 and 2009. The majority of this thesis was published in the American Journal of Physiology in 2010[1].

[1]**Orczewska JI, Hartleben G, and O'Brien KM.** The molecular basis of aerobic metabolic remodeling differs between oxidative muscle and liver of threespine sticklebacks in response to cold acclimation. *Am J Physiol Regul Integr Comp Physiol* 299: R352-364, 2010.

ACKNOWLEDGEMENTS

There are many people that have made my experience as a student very special and unforgettable. I would like to express my deepest gratitude to my major advisor Dr. Kristin O'Brien for her stimulating suggestions, precious support, constant guidance and encouragement throughout my degree. I also want to thank my committee members: Dr. Michael Harris and Dr. Thomas Kuhn for all of their advice, guidance and humor.

I would like to thank the Alaska Natives in Science and Engineering Program (ANSEP), Alfred P. Sloan Foundation and the Alaska INBRE program. Specifically, I would like to thank Dr. Dan Solie, Dr. Bill Schnabel, Dr. Thomas Clausen and Dr. Sue Hills for their unyielding support, guidance and encouragement.

I would also like to thank the Ahtna Heritage Foundation, Ahtna Corporation, Chitina Native Corporation and Alfred P. Sloan Foundation for their many years of monetary support.

I especially would like to thank my lab colleagues and close friends Irina Müller for her companionship and excellent technical help as well as Aaron Kammer for his endless discussion and humor.

I cannot express all of the affection and gratitude to my parents, siblings, extended family and boyfriend for all of their unyielding support and faith during this process.

1. INTRODUCTION

Changes in temperature pose significant challenges to fish because as ectotherms they are at thermal equilibrium with their environment. Maintaining the production of ATP as temperature declines is particularly problematic because for every 10°C reduction in temperature, there is a two- to three-fold reduction in the catalytic rate of enzymes (23). Metabolic capacity may be maintained during cold acclimation by either quantitative or qualitative changes in enzymes. The most common strategy employed by fish to maintain aerobic metabolic capacity is to elevate the concentration of rate-limiting metabolic enzymes in oxidative tissues (65, 69). Qualitative changes in enzymes brought about by expressing alternative isoenzymes requires having a larger genome and is a strategy more commonly employed by polyploid fishes (48).

Increases in aerobic metabolic capacity during cold acclimation have been documented in many fish species, yet little is known about how this process is regulated (12, 31, 41, 47, 65, 75). Aerobically-poised enzymes of the Kreb's cycle, oxidative phosphorylation and fatty-acid oxidation are localized within the mitochondrion. Consequently, increases in the concentration of aerobic metabolic enzymes during cold acclimation are often accompanied by increases in the percentage of cell volume displaced by mitochondria (12, 31, 75). In mammals, increases in mitochondrial density are brought about through the transcriptionally-regulated process of mitochondrial biogenesis (24).

Mitochondrial biogenesis is complicated because the mitochondrion houses proteins encoded in both the nuclear and mitochondrial genomes. The majority of studies of mitochondrial biogenesis have been conducted in mammals, where it has been shown that the activities of the two genomes are coordinated by the peroxisome proliferator-activated receptor gamma coactivator-1 (PGC-1) family of transcriptional co-activators which includes PGC-1α, PGC-1β, and PGC-1-related co-activator (PRC) (60). All three PGC-1 co-regulators can stimulate mitochondrial biogenesis. PRC expression is correlated with the cell cycle and induced in response to proliferative signals, suggesting it is involved in mitochondrial biogenesis during cell division (59). PGC-1α and PGC-1β

are both expressed in highly oxidative tissues, but seem to have some tissue-specific activities (19, 42, 57). PGC-1α and PGC-1β, operating along with a suite of transcription factors including peroxisome proliferator-activated receptors (PPARs), estrogen-related receptors (ERRs), Yin yang 1(YY-1), cAMP response element-binding protein (CREB), c-Myc and nuclear respiratory factor-1 and -2 (NRF-1 and NRF-2), induce the expression of nuclear-encoded genes destined for the mitochondrion, including ones involved in oxidative phosphorylation, heme biosynthesis, mitochondrial protein import and the assembly of multimeric proteins (24, 61). Importantly, the activity of the nuclear genome is linked with the mitochondrial genome by mitochondrial transcription factor-A (TFAM), which is also encoded in the nuclear genome. The expression of TFAM is induced by PGC-1α and NRFs. It is then translated on cytosolic ribosomes and imported into the mitochondrion where it transactivates the expression of mitochondrially-encoded genes involved in oxidative phosphorylation, and stimulates the replication of the mitochondrial genome (14). While mitochondrial biogenesis has been well-characterized in mammals, less is known about how mitochondrial proliferation is regulated in fish and if increases in aerobic metabolic capacity are always linked to mitochondrial biogenesis during cold acclimation.

Studies coupling quantitative analysis of mitochondrial volume density with measurements of maximal activities of aerobically-poised enzymes have revealed that mitochondrial biogenesis is a common response to cold acclimation in oxidative muscles of fish (12, 30, 31, 75). The picture is less clear in liver. Several studies have determined that the maximal activity of citrate synthase (CS) increases in response to cold acclimation, but often in the absence of an increase in the maximal activity of cytochrome c oxidase (COX), suggesting that increases in aerobic metabolic capacity may not always coincide with mitochondrial biogenesis in liver (15, 41, 44). Only in the livers of the blennie (*Blennius pholis*), has cold acclimation been shown to increase the number of mitochondria but volume density of mitochondria was not quantified (5). The oxygen consumption rate per g liver tissue measured at the common temperature of 15°C was two-fold higher in striped-bass (*Morone saxatilis*) acclimated to 5°C compared to

those at 25°C, suggesting that either mitochondrial densities or the activity of individual mitochondria increased in response to cold acclimation (70). The oxygen consumption rate per g tissue of liver was unaffected by cold acclimation in eels (*Anguilla anguilla*), but the hepatosomatic index, the ratio of liver mass to the body weight, increased, suggesting liver function was maintained at cold temperature by hepatocyte proliferation (29). It is not surprising that tissues respond differentially to cold acclimation given their diverse metabolic requirements (65). Nevertheless, little is known about how tissue-specific responses to cold acclimation are regulated.

Only two studies to date have examined the potential role of PGC-1 family members and NRFs in regulating increases in aerobic metabolic capacity in response to cold acclimation in fish. Results from these studies suggest that the regulatory pathway leading to increases in aerobic metabolic capacity differ between fish and mammals. In goldfish (*Carassius auratus*), cold acclimation resulted in a significant increase in the maximal activity of CS in oxidative and glycolytic muscle, and a corresponding increase in mRNA levels of NRF-1 (41). Similar results were also found in glycolytic muscle of zebrafish (*Danio rerio*) (47). Cold acclimation also stimulated an increase in the activity of COX in oxidative and glycolytic skeletal muscles but not liver of goldfish (41). Notably, neither study detected a significant increase in transcript levels of PGC-1α in response to cold acclimation. However, in goldfish, mRNA levels of PGC-1β increased in oxidative muscle and liver, suggesting a more prominent role for this PGC-1 family member in the metabolic remodeling of fish in response to cold acclimation (41). Increases in CS and COX enzyme activity were not always correlated with increases in transcript levels of CS and COX subunits, suggesting that elements of aerobic metabolic restructuring may be post-transcriptionally regulated in fish (41, 47). No studies have coupled measurements of PGC-1 family members and NRF-1 with measurements of mitochondrial density during cold acclimation in fish, so it is unclear if these factors govern increases in aerobic metabolic capacity and/or mitochondrial biogenesis. Moreover, nothing is known about the trigger stimulating metabolic remodeling in response to cold acclimation in fish. In mammals, the expression and/or activity of PGC-

1α is induced and mitochondrial biogenesis activated by AMP-activated protein kinase, sirtuin-1, calcium, reactive oxygen species, carbon monoxide, nitric oxide and mammalian target of rapamycin (mTOR) (8, 28, 33, 39, 51, 72, 82). The first step towards identifying which, if any, of these signaling molecules stimulates metabolic remodeling during cold acclimation in fish is to identify the time frame in which metabolic remodeling occurs.

Our study sought to address several questions regarding the molecular basis of aerobic metabolic remodeling in response to cold acclimation in fish. We sought to determine: (1) if metabolic remodeling differs between liver and oxidative muscle; (2) how metabolic remodeling is regulated in each tissue; (3) the time frame for metabolic remodeling; and (4) if known regulators of mitochondrial biogenesis in mammals also play a role in aerobic metabolic remodeling of fish in response to cold acclimation. This is the first study to quantify changes in mitochondrial density in liver in response to cold acclimation using transmission electron microscopy, rather than relying on measurements of aerobic metabolic enzymes as proxies for mitochondrial density. In addition, it is the first study to measure the activity of aerobic metabolic enzymes, transcript levels of aerobic metabolic enzymes and transcript levels of genes known to regulate mitochondrial biogenesis during the time course of cold acclimation. This provides a comprehensive examination of the molecular basis of aerobic metabolic remodeling and allows us to identify when changes in aerobic metabolic capacity occur so that we may ultimately identify the trigger of aerobic metabolic remodeling in response to cold acclimation in fish.

We used the threespine stickleback, *Gasterosteus aculeatus* in our experiments. Sticklebacks are eurythermic fishes, found in both marine and freshwater environments (81). Along the West Coast of the United States, sticklebacks range from Barrow, AK (71°N Lat) to central California (35°N Lat) in regions which experience significant seasonal changes in temperatures. In lakes of central Alaska, where the animals used in this study were collected, water temperatures range from 23°C to 4°C during the year. Given their diverse thermal habitats, we anticipated sticklebacks possessed the genetic

capacity to acclimate to changes in temperature. Consistent with this prediction, previous studies have shown that sticklebacks undergo metabolic remodeling in response to temperature acclimation (76). Additionally, sticklebacks are the only eurythermic fish whose genome has been sequenced, making molecular biological studies more straightforward compared to non-model fish species.

2. MATERIALS AND METHODS

2.1 Animals.

The use of animals was approved by the University of Alaska Fairbanks Institutional Animal Care Committee (135490-2). 350 threespine stickleback (*Gasterosteus aculeatus*) were collected from Kashwitna Lake, AK (61°50'N, 150° 00'W) using minnow traps in August, 2007 when the water temperature was 16.5°C. By this time of year, animals had already spawned. Fish were transported to the University of Alaska Fairbanks where they were maintained in 114 L aquaria filled with aerated, filtered water supplemented with Instant Ocean (0.35%). Animals were held at 20°C for 12 weeks on a 10 hr light, 14 hr dark cycle to inhibit reproductive activity. Fish were fed *ad libitum* twice daily a diet of blood worms and brine shrimp. After 12 weeks at 20°C, 38 individuals were harvested. The remaining animals were either acclimated to cold temperature (8°C) or maintained at 20°C for an additional 9 weeks. For cold acclimation, the room temperature was decreased from 20°C to 15°C on day one, from 15°C to 10°C on day two, and to 8°C on day three (Fig. 1). The water temperature was decreased by a rate of 0.35°C per hour each day until the desired temperature was reached. 30-40 animals were harvested each day prior to decreasing the temperature and again after 1, 4 and 9 weeks at 8°C.

Animals were euthanized with an overdose of MS 222 for measurements of cell size, ultrastructural characteristics and the maximal activity of cytochrome c oxidase (COX). For measurements of the maximal activities of citrate synthase (CS), mitochondrial DNA (mtDNA) and mRNA levels, animals were frozen in liquid nitrogen

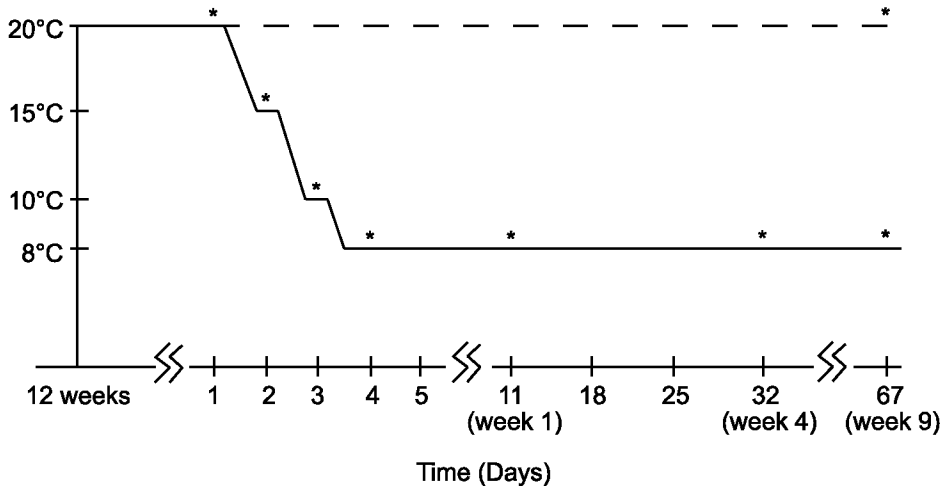

Fig. 1. Experimental Design. Stickleback were held at 20°C for 12 weeks. One group of warm-acclimated fish (N = 30) was held at 20°C for an additional 9 weeks. The second group of ~240 fish was cold acclimated by decreasing the temperature in the environmental chamber where tanks were held to 15°C, then 10 ºC and then 8°C over a three day period. Animals were then maintained at 8°C for an additional 9 weeks. 30-40 animals were harvested at each time point designated by an asterisk.

and stored at -80°C. All animals were harvested at the same time each morning, prior to feeding to avoid the potentially confounding effects of circadian rhythms on gene expression (56). Different groups of animals were used for measuring cell size and ultrastructural characteristics, enzyme activity, gene expression and mtDNA copy number because of the small size of sticklebacks. Body mass, length, and masses of liver and oxidative muscles were measured in each individual.

2.2 Measurements of cell size and ultrastructural characteristics.

Oxidative pectoral adductor muscle and liver tissues were excised from 6 fish held at 8°C and 20°C for 9 weeks. Tissues were fixed on ice in 0.1 M sodium cacodylate, 1% glutaraldehyde, 4% formaldehyde, 7.5% sucrose and 2 mM $CaCl_2$ for at least 2 hours. The pectoral adductor muscle was left attached to the underlying cartilage during this initial fixation step. Tissues were then diced into 1 mm-sized cubes, rinsed in buffer (0.1 M sodium cacodylate, 7.5% sucrose and 2 mM $CaCl_2$, pH 7.5) and stored overnight at 4°C. The following day, tissues were rinsed in fresh buffer (0.1 M sodium cacodylate, 7.5% sucrose and 2 mM $CaCl_2$, pH 7.5) for 20 minutes on ice and post-fixed for 1 hour on ice in 0.1 M sodium cacodylate, 1% OsO_4 and 2 mM $CaCl_2$, pH 7.5. Tissues were rinsed in Milli Q H_2O and dehydrated through a series of increasing concentrations of acetone (70%, 95%, 100%) and embedded in a mixture of Epon and Araldite (Ted Pella, Redding, CA).

Semi-thin sections (0.5 – 1.5 μm) were cut using a Sorvall JB4 microtome and stained with 1% toluidine blue in 1% borax. Sections were viewed using a Nikon Eclipse 80i upright microscope equipped with a QImaging Micropublisher 3.3 camera. Images were captured at a final magnification of 40X for oxidative muscle and 100X for liver tissue using the software Metamorph Ver. 7.1.2.0 (Molecular Devices). The cross-sectional area of 40 oxidative muscle fibers and 80 hepatocytes was measured in 4-6 individuals using ImageJ Ver. 1.42q (National Institutes of Health).

Volume and surface densities were quantified using electron microscopy and sterological methods (78). Ultra-thin sections (~ 80 nm) were cut using a Leica EM UC6

ultramicrotome, collected on 200-mesh copper grids and stained with 2% uranyl acetate followed by 0.5% lead citrate. Sections were viewed with a JEOL-1200EX transmission electron microscope fitted with an AMT digital camera. 15-20 micrographs were taken from each of 3-4 individuals using the aligned-systematic-quadrats-subsampling method (7). Measurements were taken at a final magnification of 12,360X in oxidative muscle and at 23,470X in liver tissue. Images were overlaid with a square lattice test pattern with spacing equal to 0.81 μm for oxidative muscle and 0.64 μm for liver tissue. Volume density was quantified using the point-counting method and mitochondrial surface density was measured using the line-intercept technique (77).

2.3 Enzyme activity.

The maximal activity of CS and COX was measured in crude homogenates of oxidative pectoral adductor muscle and liver tissue from 4-6 individuals harvested at each time point during acclimation. Assays were carried out in triplicate at 10°C (CS) or 14°C (COX) using a Perkin Elmer Lambda 25 spectrophotometer equipped with a temperature-controlled circulating water bath.

Citrate synthase (EC 2.3.3.1). The maximal activity of CS was measured as described previously (52). Tissues were homogenized by hand in a ground glass homogenizer in 10 volumes of ice-cold buffer (250 mM Tris-HCl, 10 mM EDTA, 10 mM EGTA, pH 7.4). The final reaction mixture contained 0.25 mM 5,5'-dithiobis-2-nitrobenzoic acid (DTNB), 0.4 mM acetyl CoA, 0.5 mM oxaloacetate, and 75 mM Tris-HCl, pH 8.0. Background activity was measured for 5 minutes in the absence of the initiating substrate oxaloacetate. The progress of the reaction was monitored by following the production of the reduced anion of DTNB at 412 nm for 5 minutes following the addition of oxaloacetate.

Cytochrome c oxidase (EC 1.9.3.1). The maximal activity of COX was measured by monitoring the oxidation of reduced cytochrome c at 550 nm (79). Tissues were

homogenized in 10 volumes of ice-cold buffer (50 mM K_2HPO_4/KH_2PO_4, 0.05% Triton X-100, pH 7.5). The final reaction mixture contained 0.07% (w/v) reduced cytochrome c in 10 mM phosphate buffer. Cytochrome c was reduced by adding 1.25 mg ml^{-1} ascorbate to a 1% (w/v) solution of cytochrome c in 10 mM^{l} phosphate buffer, pH 7.5. Ascorbate was removed by dialysis against 10 mM phosphate buffer, pH 7.5. Reduced cytochrome c was stored in liquid N_2 until use. Its reduction state was verified by measuring the 550 nm : 565 nm absorbance ratio to ensure that it was always > 8. The reaction was initiated by the addition of enzyme.

2.4 RNA isolation.

RNA was isolated from 10-30 mg of oxidative pectoral adductor muscle and liver tissue from 6-12 individuals harvested at each time point during acclimation using the RNeasy Fibrous Tissue Mini-kit (Qiagen). Liver lysates were not treated with proteinase K and slight modifications were made to the manufacturer's protocol to improve the removal of genomic DNA. RNA was treated twice with DNase, once for 25 minutes and a second time for 20 minutes. RNA was eluted with 30 µl of RNase-free water, pH 8.0 and then reapplied to the column to elute any remaining RNA. RNA levels were quantified by measuring the absorbance at 260 nm with a Nano-Drop® (ND-1000) spectrophotometer. RNA purity was determined by measuring the 260 : 280 absorbance ratio and only samples with a ratio greater than 1.8 were used for measuring gene expression. RNA integrity was verified by agarose electrophoresis. 2 µl of RNA was mixed with loading buffer (5% glycerol, 0.04% bromophenol blue, 0.1 mmol l^{-1} EDTA, pH 8.0) and separated on a 2% agarose gel. RNA was stored at -80°C.

Complementary DNA (cDNA) was synthesized using TaqMan® reverse transcription reagents (Applied Biosystems). Each 10 µl reaction contained 5.5 mM $MgCl_2$, 2.5 µM random hexamers, 2 mM dNTPs, 4 U of RNase inhibitor, 37.5 U reverse transcriptase and 200 ng RNA. Synthesis reactions were performed using an iCycler (Bio-Rad Laboratories) programmed at 25°C for 10 minutes, 48°C for 30 minutes and 95°C for 5 minutes.

2.5 Gene expression.

Transcript levels of CS, COXIII, COXIV, PGC-1α, PGC-1β, NRF-1 and TFAM were measured in animals harvested throughout the warm- and cold-acclimation period using quantitative real-time PCR (qRT-PCR). Gene-specific primers were designed using sequence information obtained from Ensembl (www.ensembl.org) and the software Primer Express (Applied Biosystems) with at least one primer from each pair spanning a splice site to ensure that genomic DNA was not amplified (Table 1, Appendix B, 11.4). Primers were synthesized commercially (Invitrogen). Transcript levels were measured in triplicate in a 20 µl reaction volume containing 5 ng cDNA, 10 µl Power SYBR® Green Master Mix (Applied Biosystems) and 0.3 µM of each forward and reverse primer. Reactions were carried out using an ABI 7900HT sequence detection system (Applied Biosystems) set to 50°C for 2 minutes and 95°C for 10 minutes followed by 40 cycles of 95°C for 15 seconds and 60°C for 1 minute. The critical threshold (Ct) value was determined within the logarithmic phase of the amplification curve. Reaction efficiency and relative quantity of input RNA were determined using a standard curve. Each standard curve was prepared by pooling and then serially diluting cDNA from 4 individuals harvested at each time point during warm- and cold- acclimation. Serial dilutions were analyzed by qRT-PCR on the same plate as samples and the logarithmic of the concentration of cDNA was plotted against the resulting Ct values. The standard curve was generated as the linear regression line through the data points (11). Separate standard curves were prepared for each gene and tissue type. A dissociation curve was run for each reaction at 95°C for 15 seconds, 60°C for 15 seconds, and 95°C for 15 seconds (slow ramp) to verify the specificity of each primer set. Two types of controls were used, one for each primer set in which the cDNA template was replaced with an equal volume of Milli Q H_2O. The second control, which was run in parallel with each sample, contained template from the cDNA synthesis reactions in which the reverse transcriptase was omitted. Both of these controls allowed us to identify and omit samples containing contaminating genomic DNA.

Table 1. Primers used for quantitative real-time PCR

Gene (Ensembl ID ENSGACG000000)	Forward Primer (5' to 3')	Reverse Primer (5' to 3')	Amplicon, bp
18S (21793)	ACCACATCCAAGGAAGGCAG	CCGAGTCGGGAGTGGGTAAT	51
ACTB (07836)	CCCCCCTGAACCCCAA	GTCTCGAACATGATCTGGGTCA	55
COXIII (20942)	CACCACACACCCCCAGTACA	GAATAGAATTATACCGTAGCGAAGGC	51
COXIV (15963)	GTGCCTGGGCTGCTCTCTC	TGATGCGGTACAATGCAATCTT	51
CS (10851)	GTTCACTGAGCTAATGCGGCT	CCTTCGTGGTCACTGTGGATG	51
CYC (11687)	TTTTTCATACACGGACGCCA	TCGAGCCTCGTGAACTGACC	51
EF-1α (02143)	CGTCTACAAAATCGGAGGTATTGG	GTCTCAACACGGCCGACTG	53
NRF-1 (19712)	CTGCCGTAGCAACAGGAAAGA	TCGCAGTTTCCTTAGCAGACG	101
PGC-1α (19546)	AGTCTCCAAATGACCACAAGGG	GGGTTCCAGCAATCTCCACA	81
PGC-1β (16810)	CGGACGACCCATCTCTGCT	GGGCACGTTGGGAGGAGT	53
TBP (16147)	GAAGACCATTGCCCTGAGAGC	AAAACGCTTTGGGTTGTAACTCTG	52
TFAM (15427)	GAGGGAGTTGACTAACCTCGGG	GTTGAATGAAGAGCGAGGACG	52

18S, 18S rRNA; ACTB, β-actin; COX, cytochrome c oxidase; CS, citrate synthase; CYC, cytochrome c; EF-1α, elongation factor-1α; NRF-1, nuclear respiratory factor-1; PGC-1, peroxisome proliferator-activated receptor γ coactivator-1; TBP, TATA-box-binding protein; TFAM, mitochondrial transcription factor.

2.6 Analysis of housekeeping genes.

The expression of target genes was normalized to a housekeeping gene (HKG) whose expression remained constant during cold acclimation. The expression level of four potential housekeeping genes: 18S rRNA (18S), TATA-box-binding protein (TBP), β-actin (ACTB), and elongation factor-1α (EF-1α) was evaluated in oxidative muscle and liver tissue using qRT-PCR in 8-10 fish harvested at 20°C, 20°C week 9, and 8°C week 9. All of these genes have either been used as, or proposed as suitable housekeeping genes for qRT-PCR (3, 9, 41, 47, 53). Reaction mixtures were identical to those described above with the exception that 1 ng of cDNA was used in each reaction to quantify transcript levels of 18S.

The excel-based tool *Bestkeeper*© version 1 was used to identify the most appropriate HKG. This software uses a combination of descriptive statistics and linear regression analysis (55). *Bestkeeper*© calculates the standard deviation of the Ct values for each gene, and genes having a standard deviation > 1 are excluded from the analysis. The remaining potential HKGs are subjected to pair-wise correlation analyses. Genes with a significant ($P < 0.05$) Pearson correlation coefficient (r) are used to calculate the *Bestkeeper Index*, which is the geometric mean of all Ct values from all genes. A second pair-wise linear regression analysis is then carried out between the *Bestkeeper Index* and each remaining candidate gene. The most appropriate HKGs have significant Pearson correlation coefficients ($P < 0.05$) with the *Bestkeeper Index*.

Bestkeeper© should be used with caution because genes that change in a similar fashion with experimental conditions can be highly correlated and appear as appropriate HKGs. To avoid this pitfall, we identified significant differences in HKG expression between warm- and cold-acclimated individuals using an ANOVA and *post-hoc* Tukey's Honestly Significant Difference (HSD) test. Genes that were significantly different between warm- and cold-acclimated animals ($P < 0.05$) were excluded.

2.7 Mitochondrial DNA copy number.

mtDNA copy number was quantified as a second metric of mitochondrial density. Measurements were made in oxidative pectoral adductor muscle and liver tissue from 6-8 warm-acclimated (20°C week 9) or cold-acclimated (8°C week 9) individuals using qRT-PCR. DNA was isolated using the DNeasy Blood and Tissue Kit (Qiagen) according to the manufacturer's protocol. mtDNA copy number was quantified as the ratio of the copy number of the mitochondrially-encoded gene, cytochrome c oxidase III (COXIII), to the copy number of the nuclear-encoded gene, cytochrome c (CYC). Reactions were prepared as described above with the exception that 5 ng DNA was used as template in each reaction.

2.8 Statistical analyses.

All statistical tests were conducted using the software JMP 7.0.2 (SAS). A Student's *t*-test was used to determine significant differences in cell size, surface and volume densities, and the ratio of mtDNA-to-nuclear DNA (nDNA) between warm- and cold-acclimated fish held at 20°C for 9 weeks and 8°C for 9 weeks. Significant differences in physical characteristics, maximal activities of enzymes and gene expression among warm- and cold-acclimated fish harvested throughout the acclimation period were determined using an ANOVA followed by a *post-hoc* Tukey's HSD test. Data were log, square root or arcsin transformed as necessary to maintain assumptions of normality, which was evaluated by residual and Q-Q plots. Correlations in gene expression were determined using Pearson's product moment correlation coefficients. All statistical tests were two-sided with a significance level set at $P < 0.05$. Data are presented as the mean ± SE.

To draw conclusions regarding significant differences between warm- and cold-acclimated fish, measurements made in cold-acclimated fish harvested between day 1 and week 4 were compared to measurements made in warm-acclimated fish harvested at the start of the acclimation period, labeled as 20°C fish. Measurements made in cold-acclimated fish harvested between weeks 4 and 9 were compared to measurements made

in warm- acclimated fish harvested at week 9. Measurements made in cold-acclimated fish harvested at week 4 were compared to both groups of warm-acclimated animals, since this time point was approximately halfway between the time points at which we harvested each group of the warm-acclimated fish.

2.9 Glycolytic muscle.

All of the previously described methods, omitting cell architecture, were also performed in the glycolytic skeletal muscle of threespine stickleback during cold acclimation. Although the results are not presented herein, they have been included in Appendix A.

3. RESULTS

3.1 Physical characteristics.

Length, body mass, and the hepatosomatic index of fish increased during the experimental period (Table 2). However, there was no effect of temperature on any of these parameters. Body mass, length and the hepatosomatic index were equivalent between warm- and cold- acclimated fish at week 9. The pectoral-to-body-mass ratio and condition index were also equivalent between cold- and warm- acclimated animals at week 9 ($P < 0.05$) (Table 2).

3.2 Changes in cell architecture in response to cold acclimation.

The size of oxidative muscle fibers did not change in response to cold acclimation but the cross-sectional area of liver cells decreased 1.4-fold (Table 3, Fig. B.1). Mitochondrial volume density significantly increased 1.9-fold in oxidative muscle in response to cold acclimation but did not change in liver (Fig. 2; Table 3). Similarly, the surface density of mitochondria significantly increased in oxidative muscle but not liver (Table 3). The mitochondrial surface-to-volume ratio remained unchanged in response to cold acclimation in oxidative muscle, indicating that the increase in mitochondrial

Table 2. Effect of cold acclimation on physical characteristics of *G. aculeatus*

Temperature and time point of harvest (N)	Length (cm)	Body mass (g)	Condition factor	Pectoral-to-body mass ratio	Hepatosomatic index
20°C (29)	5.03 ± 0.07‡	1.24 ± 0.05‡	0.96 ± 0.02‡	0.016 ± 0.001	4.72 ± 0.17
15°C (14)	5.18 ± 0.11‡	1.39 ± 0.07‡	1.00 ± 0.04	0.015 ± 0.001	4.91 ± 0.34
10°C (16)	5.29 ± 0.10‡	1.60 ± 0.09‡*	1.06 ± 0.04	0.017 ± 0.001	5.06 ± 0.33
8°C (18)	5.31 ± 0.08‡	1.78 ± 0.08*	1.18 ± 0.02‡*	0.017 ± 0.001	5.08 ± 0.44
8°C wk 1 (16-18)	5.34 ± 0.07‡	1.69 ± 0.08*	1.12 ± 0.04*	0.015 ± 0.001	6.42 ± 0.29*
8°C wk 4 (14)	5.44 ± 0.06*	1.75 ± 0.06*	1.08 ± 0.03	0.016 ± 0.001	6.25 ± 0.26*
8°C wk 9 (26)	5.85 ± 0.05*	2.10 ± 0.06*	1.05 ± 0.02	0.017 ± 0.001	6.07 ± 0.20*
20°C wk 9 (24)	5.71 ± 0.08*	1.97 ± 0.07*	1.06 ± 0.03	0.017 ± 0.001	5.89 ± 0.17*

Condition factor = 100 * (body mass (g) * length (cm) $^{-3}$). Hepatosomatic index = 100 * (liver mass (g) * body mass (g) $^{-1}$). Values are presented as mean ± SE. *Significantly different from animals at 20°C. ‡Significantly different from animals at 20°C week 9.

Table 3. Effect of cold acclimation on cell size and ultrastructure in *G. aculeatus*

	Oxidative muscle fibers		Liver	
	20 °C wk 9	8 °C wk 9	20 °C wk 9	8 °C wk 9
$\bar{A}$ (c) μm^2	847.95 ± 69.50	880.52 ± 78.82	186.85 ± 19.36	133.00 ± 7.24*
V_v(mit,c) (%)	12.47 ± 1.75	23.74 ± 1.84*	4.85 ± 0.57	4.27 ± 0. 42
S_v(mit,c) (μm^{-1})	1.02 ± 0.17	1.65 ± 0.11*	0.57 ± 0.02	0.47 ± 0.04
Sv(mit,c): V_v(mit,c)	8.12 ± 0.42	7.05 ± 0.55	12.07 ± 1.07	10.98 ± 0.72
V_v(lip,c) (%)	0.36 ± 0.04	0.51 ± 0.14	58.67 ± 4.03	56.94 ± 8.47

Values are presented as mean ± SE (N=3-6). $\bar{A}$ (c), mean cross-sectional area of cells; Vv, fraction of cell volume occupied by mitochondria (mit,c) or lipids (lip,c); Sv(mit,c), surface density of mitochondria; Sv(mit,c) : Vv(mit,c), mitochondrial surface-to-volume ratio. *Significantly different between warm- and cold-acclimated fish within a tissue ($P < 0.05$).

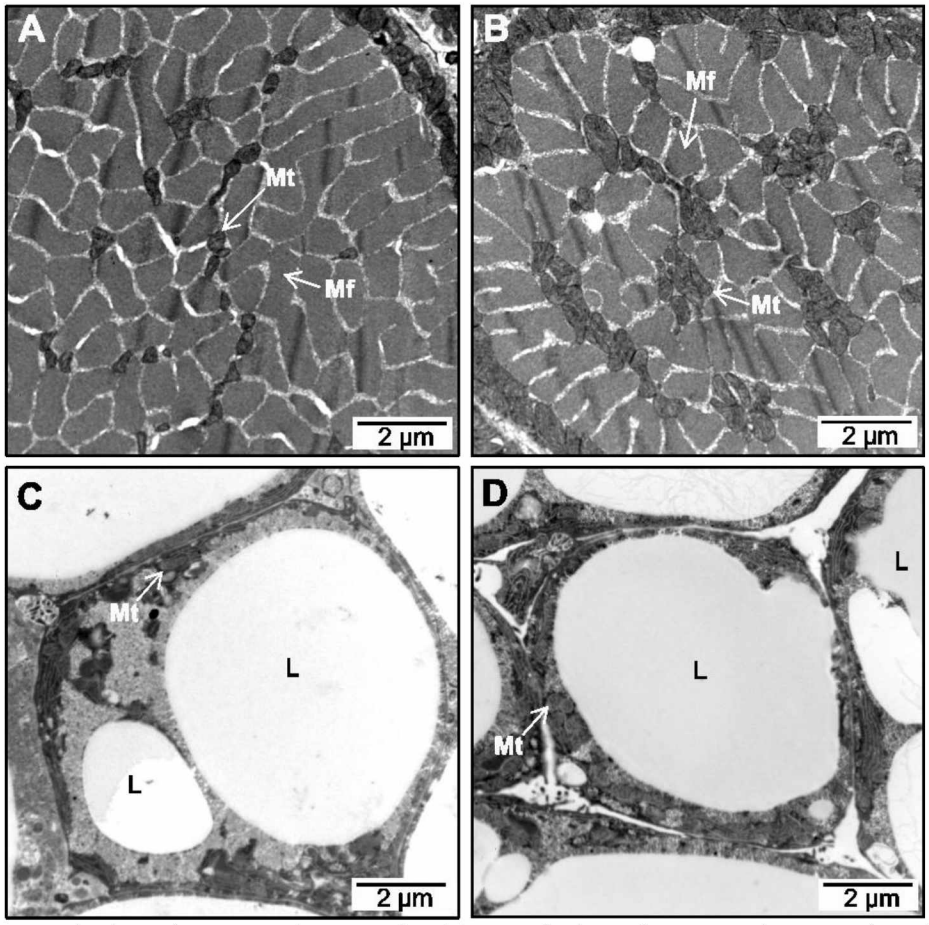

Fig. 2. Transmission electron micrographs. Transmission electron micrographs of oxidative muscle fibers (A and B) and liver tissue (C and D) from warm- (A and C) and cold- (B and D) acclimated stickleback held at 20°C for 9 weeks and 8°C for 9 weeks. L, lipid; Mf, myofibril; Mt, mitochondria.

volume density was due to mitochondrial proliferation and not an increase in organelle size (Table 3).

The ratio of mtDNA-to-nuclear DNA was measured as a second metric of mitochondrial content. The mtDNA-to-nDNA ratio increased 1.6-fold in liver tissue but did not change in oxidative muscle in response to cold acclimation ($P < 0.05$) (Fig. 3).

3.3 Time course for metabolic remodeling in response to cold acclimation.

The time course for metabolic remodeling was assessed by measuring the maximal activity of two aerobically-poised enzymes, CS and COX during cold acclimation. The maximal activity of both CS and COX increased in response to cold acclimation in oxidative muscle and liver tissue (Fig. 4). The maximal activity of CS did not significantly increase in oxidative muscle until animals had been maintained at 8°C for 9 weeks. At that point, the maximal activity of CS activity had increased 1.7-fold compared to fish at 20°C for 9 weeks ($P < 0.05$) (Fig. 4A). The maximal activity of COX increased early during cold acclimation in oxidative muscle, and was significantly higher in animals on day 1 at 8°C compared to animals at 20°C ($P < 0.05$) (Fig. 4A). COX activity increased 1.9-fold in oxidative muscle by week 9 of cold acclimation compared to animals at 20°C for 9 weeks ($P < 0.05$) (Fig. 4A).

The maximal activity of CS significantly increased in liver after 1 week at 8°C compared to animals at 20°C (Fig. 4B). The maximal activity of CS was 2.0-fold higher in animals after 9 weeks at 8°C compared to those at 20°C for 9 weeks ($P < 0.05$). The maximal activity of COX did not increase in liver until animals were cold-acclimated to 8°C for 9 weeks, at which point COX activity was 1.5-fold higher compared to animals at 20°C for 9 weeks ($P < 0.05$) (Fig. 4B).

3.4 Identification of a stable housekeeping gene.

The stability of four potential housekeeping genes (18S, ACTB, TBP, EF-1α) was analyzed in the oxidative pectoral adductor muscle and liver tissue of warm- (20°C and 20°C week 9) and cold-acclimated fish (8°C week 9). In oxidative muscle, the

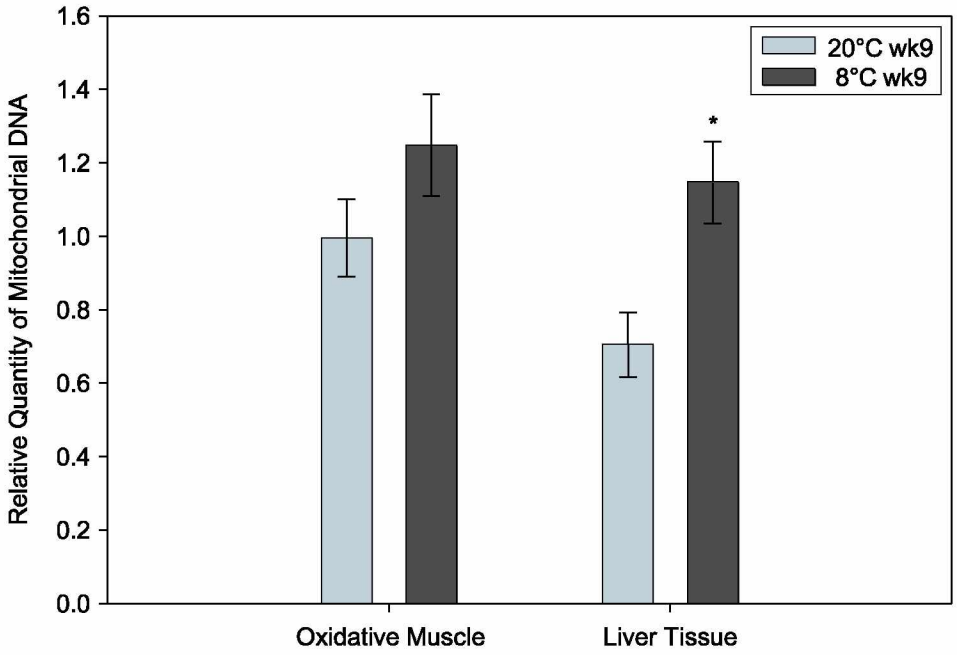

Fig. 3. Changes in mitochondrial DNA copy number. The ratio of mitochondrial DNA-to nuclear DNA was quantified by measuring levels of the mitochondrially-encoded gene COXIII and the nuclear-encoded gene CYC in oxidative muscle and liver tissue in animals held at 8°C for 9 wk and 20°C for 9 wk. (N=6-8). Values are presented as means ± SE *Indicates a significant difference within a tissue ($P < 0.05$).

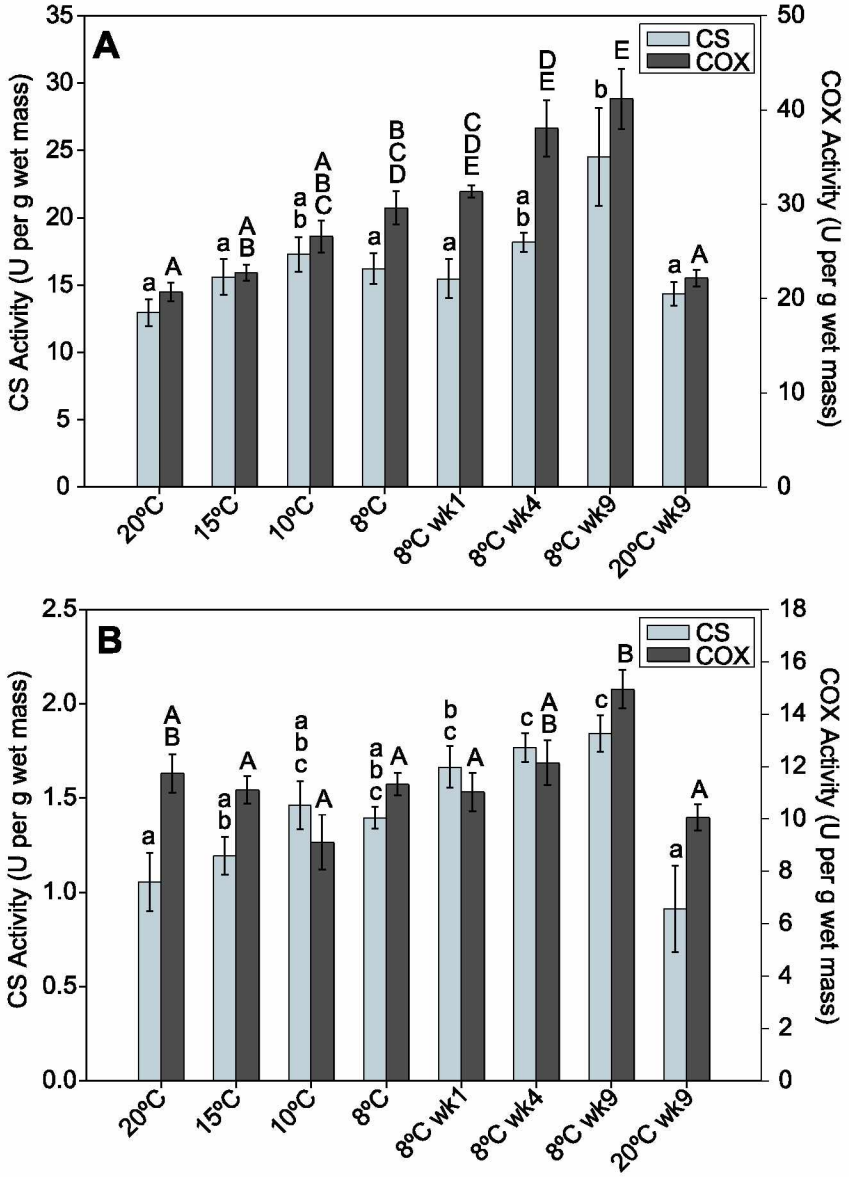

Fig. 4. Maximal activity of aerobic metabolic enzymes. The maximal activity of CS and COX was measured at a common temperature in oxidative muscle (A) and liver tissue (B) during cold acclimation. Values are presented as means ± SE (N=4-6) Different letters within a series denote significant differences among warm- and cold-acclimated fish ($P < 0.05$). CS, citrate synthase; COX, cytochrome c oxidase.

standard deviation of all of the HKGs was < 1.0 and the mRNA levels of ACTB and EF-1α were significantly correlated with the *Bestkeeper Index* (Table 4). The mRNA levels of ACTB were significantly different between warm- and cold-acclimated fish in oxidative muscle ($F < 0.05$). As a result, ACTB was excluded as a potential HKG in oxidative muscle and EF-1α was used for normalizing the expression of target genes. In liver, 18S was the only HKG with a standard deviation < 1.0 and whose expression did not differ between warm- and cold- acclimated fish (Table 4).

3.5 Changes in the expression of aerobic metabolic genes in response to cold acclimation.

CS mRNA levels were higher in oxidative muscle of animals at week 4 of cold acclimation compared to those at 20°C for 9 weeks but not compared to animals at 20°C at the start of the experiment (Fig. 5A). By week 9 of cold acclimation, transcript levels of CS were significantly elevated in oxidative muscle compared to both control groups ($P < 0.05$). This coincided with an increase in CS activity (Fig. 4A). In liver tissue, CS expression was 4.1-fold higher in animals at 10°C compared to animals at 20°C ($P < 0.05$) (Fig. 5B). The increase in CS mRNA levels was detected 8 days prior to the increase in CS activity in liver (Fig. 4B). CS mRNA levels then decreased by week 4 of cold acclimation in liver, although CS activity remained elevated (Fig. 5B and 4B). Transcript levels of the nuclear- and mitochondrial-encoded subunits (COXIV and COXIII, respectively) of COX were measured during cold acclimation. In oxidative muscle, mRNA levels of COXIV were significantly higher in animals at 8°C for 9 weeks compared to those at 20°C for 9 weeks (Fig. 5C). The increase in expression of COXIV occurred 9 weeks after the increase in the maximal activity of COX (Fig. 4A). There was no significant change in the expression of COXIII with cold acclimation in oxidative muscle ($P > 0.05$) (Fig. 5C). In liver tissue, neither the expression of COXIII nor COXIV changed in response to cold acclimation (Fig. 5D).

Table 4. Housekeeping gene analysis using Bestkeeper©

Gene	Oxidative muscle				Liver			
	SD	r	P-value for r	F-value for ANOVA	SD	r	P-value for r	F-value for ANOVA
18S	0.64	0.139	0.516	0.245	0.93	0.791	0.001	0.084
ACTB	0.99	0.577	0.003	0.019	1.38	0.881	0.001	0.0003
EF-1α	0.51	0.6	0.003	0.094	1.12	0.886	0.001	0.01
TBP	0.72	0.527	0.223	0.351	1.21	0.906	0.001	0.002

SD, Standard deviation of critical threshold (Ct) values; r, Pearson correlation coefficient comparing Ct values of selected housekeeping genes with the *Bestkeeper Index*. N=8-10.

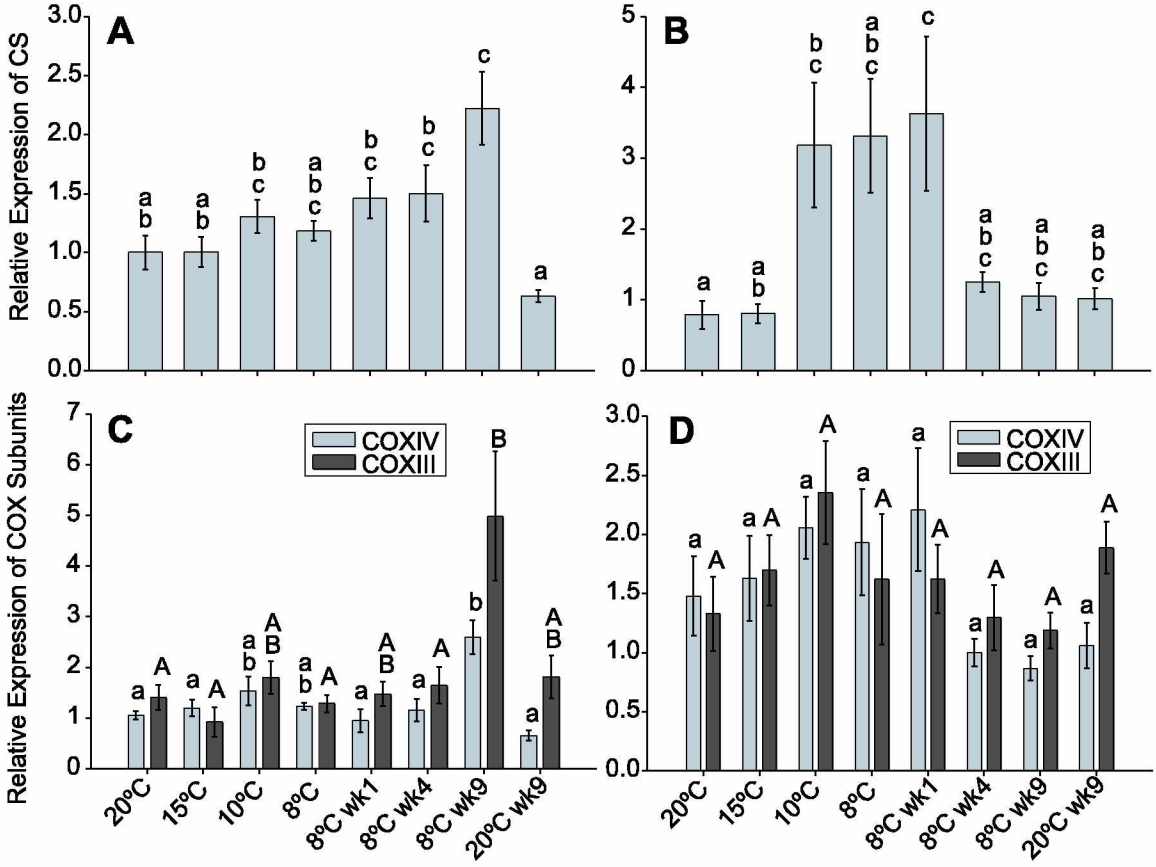

Fig. 5. Transcript levels of aerobic metabolic genes. Levels of the nuclear-encoded aerobic metabolic genes CS and COXIV, and the mitochondrially-encoded gene COXIII, were quantified in oxidative muscle (A and C) and liver (B and D) using qRT-PCR. mRNA levels were normalized to EF-1α in oxidative muscle and 18S rRNA in liver. Values are presented as means ± SE (N=5-8). Different letters within a series denote significant differences within a tissue among cold- and warm-acclimated fish ($P < 0.05$). CS, citrate synthase; COX, cytochrome c oxidase.

3.6 Changes in the expression of genes involved in regulating mitochondrial biogenesis in response to cold acclimation.

There was no significant increase in the transcript levels of either PGC-1α or PGC-1β in response to cold acclimation in oxidative muscle (Fig. 6A). The mRNA levels of NRF-1 increased in the oxidative muscle of animals after 9 weeks at 8°C compared to animals maintained at 20°C for 9 weeks ($P < 0.05$) (Fig. 6C). Levels of TFAM mRNA did not increase in response to cold acclimation in oxidative muscle (Fig. 6E).

There was no significant change in the expression of PGC-1α during cold acclimation in liver tissue (Fig. 6B). PGC-1β transcript levels were 6-fold higher in liver tissues of animals at 10°C compared to those at 20°C ($P < 0.05$) (Fig. 6B). The transcript levels of PGC-1β remained elevated in animals for up to 1 week at 8°C (Fig. 6B). The mRNA level of NRF-1 increased in liver tissues of fish at 10°C and was also significantly higher in animals after 1 week at 8°C compared to fish at 20°C (Fig. 6D). There was a 2.8-fold increase in TFAM expression in animals at 8°C for 1 week compared to animals held at 20°C ($P < 0.05$) (Fig. 6F). The transcript levels of PGC-1β, NRF-1 and TFAM all decreased after week 1 of cold acclimation and were not significantly different between fish at 8°C for 9 weeks and 20°C for 9 weeks (Fig. 6B, 6D and 6F).

4. DISCUSSION

The results presented here provide several new insights regarding the molecular basis of metabolic remodeling in response to cold acclimation in fish. First, we determined that while the maximal activity of CS and COX increased in both liver and oxidative muscle in response to cold acclimation, mitochondrial biogenesis only occurred in muscle. Secondly, we determined that the time course and molecular basis of metabolic remodeling differed between oxidative muscle and liver. Third, we identified differences in the transcriptional and co-transcriptional activators driving metabolic remodeling between liver and oxidative muscle.

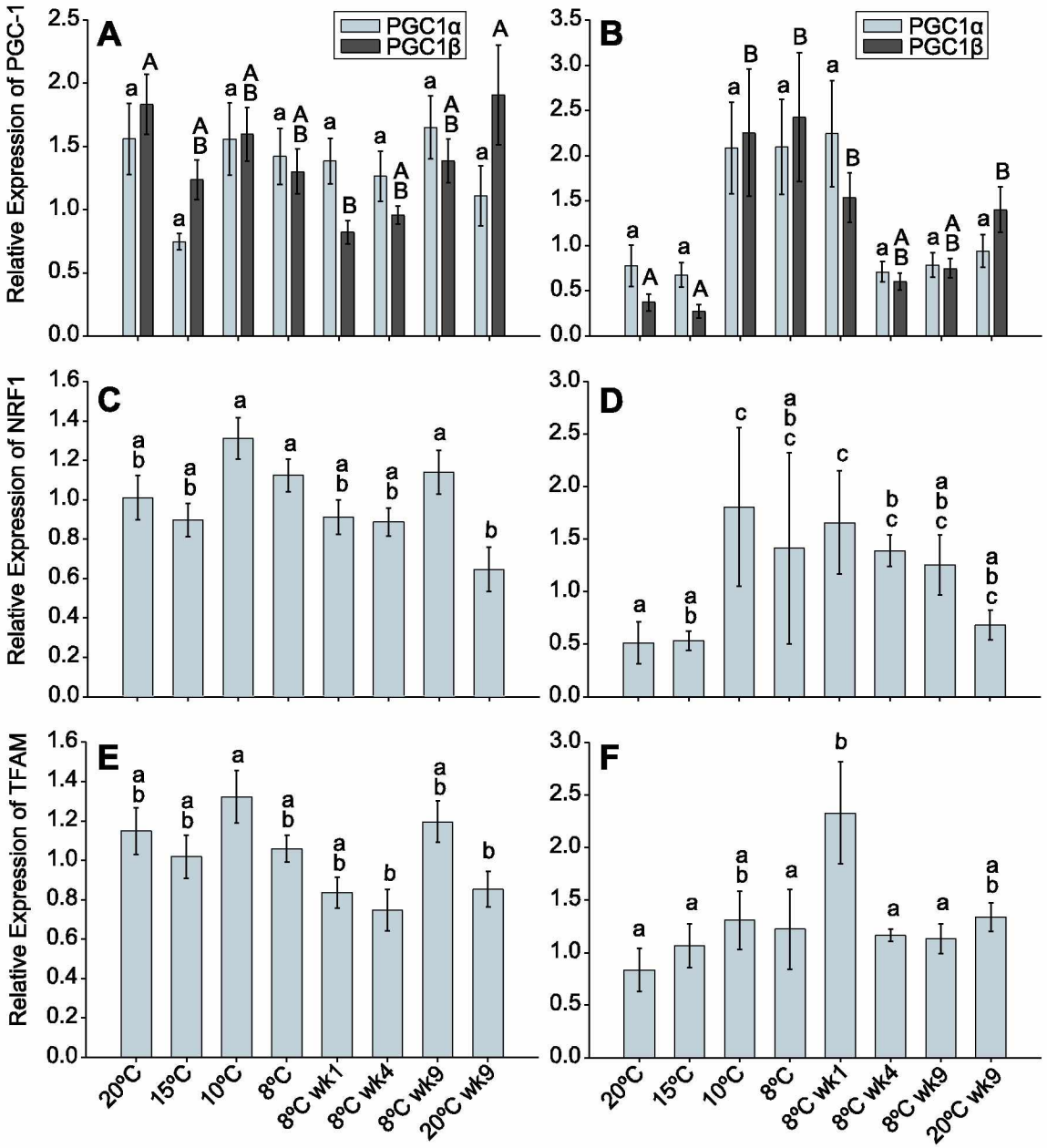

Fig. 6. Transcript levels of genes involved in regulating mitochondrial biogenesis. Gene expression was quantified using qRT-PCR. Transcript levels were normalized to EF-1α in oxidative muscle (A, C and E) and 18S rRNA in liver (B, D, and F). Values are presented as means ± SE (N=6-12). Different letters within a series denote significant differences within a tissue among cold- and warm-acclimated fish ($P < 0.05$). PGC-1, peroxisome proliferator-activated receptor γ coactivator-1; NRF-1, nuclear respiratory factor-1; TFAM, mitochondrial transcription factor A.

4.1 Metabolic remodeling in response to cold acclimation.

The maximal activity of two aerobically-poised enzymes, CS and COX increased in response to cold acclimation in both oxidative muscle and liver tissue. However, the magnitude of change in enzyme activity and the time frame in which these changes occurred differed between the two tissues. In oxidative muscle, the maximal activity of CS did not become significantly elevated until week 9 of cold acclimation. In contrast, in liver, the maximal activity of CS became significantly elevated after only 1 week of cold acclimation. The maximal activity of COX increased in oxidative muscle more rapidly compared to CS and was significantly elevated on day 3 of cold acclimation when fish had been at 8°C for < 24 hr. This rapid increase in COX activity was similar to the 1.5-fold increase in COX activity found in glycolytic muscle of killifish following 9 days of cold acclimation to 5°C compared to fish at 25°C (18). In contrast, the maximal activity of COX did not become significantly elevated in liver until week 9 of cold acclimation. The activity of CS increased to a greater degree in liver compared to muscle (2-fold vs. 1.7-fold), whereas the activity of COX increased to a greater degree in muscle compared to liver (1.9 vs. 1.5) by week 9 of cold acclimation.

The greater increase in CS activity in liver compared to COX in response to cold acclimation is consistent with findings from several other studies. Elevations in CS activity were observed in the absence of increases in COX activity in liver during cold acclimatization in chain pickerel (*Esox niger*), and cold acclimation in eelpout (*Zoarces viviparous*), killifish, and goldfish (15, 36, 41, 44). The greater increase in CS compared to COX in liver may reflect a greater anabolic demand in liver during cold acclimation. Intermediates in the Kreb's cycle are used in the synthesis of amino acids, fatty acids, purines, pyrimidines and heme (46) and some intermediates, including citrate, oxoloacetate and succinate function as antioxidants (58). Cold acclimation increases oxidative damage in livers of sea bream (27). Similarly, we found higher levels of oxidative stress in stickleback livers compared to muscle during cold acclimation (32). An increase in oxidatively damaged proteins and nucleic acids may require an increase in anabolic pathways to replace damaged macromolecules.

Increases in the maximal activity of CS and COX coincided with an increase in mitochondrial volume density in oxidative muscle, but not in liver. These differences may be due to differing metabolic demands and/or tissue architecture. There are two benefits to expanding mitochondrial populations during cold acclimation. First, high mitochondrial densities increase the concentration of aerobic metabolic enzymes per gram of tissue, compensating for the depressive effect of cold temperature on the catalytic rate of enzymes. Secondly, high mitochondrial densities compensate for the negative effect of cold temperature on the diffusion rate of metabolites and oxygen (66). Increased mitochondrial densities decrease the diffusion distance for metabolites and oxygen between capillaries and mitochondria. Additionally, oxygen is more soluble within the hydrocarbon core of mitochondrial membranes compared to the aqueous cytosol, making mitochondrial membranes a low-resistance pathway for the intracellular diffusion of oxygen (71).

Elevations in aerobic metabolic capacity in stickleback livers were achieved by increasing the concentration of enzymes within each mitochondrion, particularly CS, rather than through mitochondrial biogenesis. CS and other enzymes of the Kreb's cycle are localized within the mitochondrial matrix. Increased enzyme concentrations may be accommodated more easily within this space compared to the protein-rich inner-mitochondrial membrane where components of oxidative phosphorylation are localized (63). The modest increase in COX activity observed in liver may be achieved through alterations in mitochondrial membrane phospholipid composition and/or post-translational modifications rather than mitochondrial biogenesis (16, 22, 80). Mitochondrial biogenesis may also not be necessary in liver if molecular diffusion is not severely limited at cold temperature. Notably, 57-59% of the cell volume of liver is occupied by neutral lipid droplets in stickleback. This is consistent with the major function of the liver as a caloric reserve, but offers the additional benefit of enhancing intracellular oxygen diffusion (10, 66). High intracellular lipid densities may offset the need to proliferate mitochondrial membranes during mitochondrial biogenesis to maintain intracellular oxygen diffusion. The size of liver cells decreased in response to

cold acclimation and liver cells are smaller compared to muscle cells, which might also minimize the need to compensate for temperature-induced limitations on metabolite diffusion through mitochondrial biogenesis.

Interestingly, changes in the copy number of mtDNA did not correlate with changes in mitochondrial volume density in either liver or oxidative muscle during cold acclimation. In oxidative muscle, mtDNA copy number remained the same despite an increase in mitochondrial volume density, whereas in liver, mtDNA copy number increased in the absence of an increase in mitochondrial volume density. Similarly, cold acclimation of rainbow trout (*Oncorhynchus mykiss*) led to an increase in CS and COX activity but not mtDNA copy number in glycolytic or oxidative skeletal muscle (1). Moreover, while CS activity reflects differences in oxidative capacity between red and white muscle in rainbow trout, copy number of mtDNA does not and is similar between the two muscle types (40). Little is known about what regulates mtDNA copy number and its turnover rate (6, 49). Mammalian somatic cells possess 100-10,000 copies of mitochondrial DNA per cell, an amount in excess of levels required to maintain gene transcription and translation (49). Consequently, mtDNA copy number does not always increase in response to conditions that stimulate mitochondrial biogenesis (68), mitochondrial DNA transcription (45) or translation (37). Although some proteins such as TFAM are involved in both mitochondrial DNA replication and transcription, some transcription factors and polymerases are specific to each process, so that mtDNA replication and transcription can be independently regulated under some conditions (14). One example is in response to oxidative stress. In yeast, reactive oxygen species (ROS) oxidatively modify the origins of replication within mtDNA, stimulating mtDNA replication independently of mitochondrial biogenesis (26). In mammals, ROS production is positively correlated with mtDNA copy number among different mtDNA haplotypes having similar rates of respiration (50). Similarly, the 1.6-fold increase in mtDNA copy number in liver tissue that occurs independently of mitochondrial biogenesis in response to cold acclimation may be due to an increase in oxidative stress that we have observed in liver (32). Together, our results suggest that measurements of

aerobic metabolic enzymes or mtDNA copy number alone should be used with caution to draw conclusions about changes in mitochondrial density in fish during cold acclimation.

4.2 The molecular basis of metabolic remodeling.

The maximal activities of CS and COX increased at different time points during cold acclimation in both liver and oxidative muscle, suggesting that their activity is differentially regulated. In oxidative muscle, the activity of COX increased 9 weeks prior to an increase in mRNA levels of the nuclear-encoded subunit, COXIV. The expression of the mitochondrially-encoded subunit, COXIII remained constant during cold acclimation. In liver tissue the activity of COX increased by week 9 of cold acclimation but neither the expression of COXIII nor COXIV changed. These results suggest that the activity of COX is post-transcriptionally regulated and that the expression of the nuclear- and mitochondrial-encoded COX subunits is not coordinately regulated.

It is not surprising that the regulation of COX activity is complicated given its complex structure (24). COX is composed of 13 polypeptide chains, two cytochromes and two copper atoms. Three subunits (COXI, COXII and COXIII) are encoded in the mitochondrial genome, and the remaining 10 are encoded in the nuclear genome (63). Similar to our results, studies of rainbow trout found that the activity COX significantly increased in response to cold acclimation in oxidative and glycolytic muscle in the absence of changes in mRNA levels of the mitochondrially-encoded subunit COXI (1). In goldfish there was a correlation between COX activity and transcript levels of COXIV but not COXI in response to cold acclimation (41). And in arctic cod, there was no increase in the mRNA level of COXII in glycolytic muscle despite an increase in COX activity in response to cold acclimation (43). Together, these results suggest that transcript levels of mitochondrially-encoded subunits of COX do not limit the activity of the holoenzyme in cold-acclimated fish.

The increase in the maximal activity of COX during cold acclimation in oxidative muscle and liver may be regulated by post-transcriptional mechanisms. COX is a multimeric protein, requiring > 20 proteins to assemble the holoenzyme (35). Alterations

in any of these proteins may impact COX activity. COX activity is also regulated by phosphorylation (22) and the lipid environment, particularly cardiolipin (38, 54, 64, 80). Membrane remodeling, resulting in an increase in the proportion of unsaturated fatty acids and alterations in phospholipid head groups, maintains membrane fluidity and the activity of integral membrane proteins during cold acclimation (20). Previous studies have determined that some changes in membrane composition occur very rapidly during cold acclimation in fish. Changes in the phospholipid head groups of kidney plasma membranes occur within 8-24 hours of cold acclimation in rainbow trout (21). The activity of Δ9-desaturase, which incorporates a double bond into membrane fatty acids, and enhances membrane fluidity, increased within one day of cold acclimation in carp (*Cyprinus carpio*) (74). Mitochondrial membrane composition changed within 9 days of cold acclimation in killifish and was correlated with a significant increase in COX activity (18). Thus, changes in COX activity in both liver and oxidative muscle of stickleback during cold acclimation occur within the time frame of membrane remodeling in other fish, suggesting a plausible mechanism for increasing aerobic metabolic capacity without altering gene transcription.

Although the activity of COX was primarily post-transcriptionally regulated during cold acclimation in stickleback, our data suggest that increases in the activity of CS were in-part transcriptionally regulated. In oxidative muscle, both CS activity and mRNA levels increased at week 9 of cold acclimation. Transcript levels of CS increased in liver on day 2 of cold acclimation (at 10°C), prior to an increase in CS activity, which occurred at week 1. Similarly, CS activity and mRNA levels both increased in response to cold acclimation in the liver and muscle of northern killifish and in livers of goldfish (15, 41). Interestingly, transcript levels declined after week 1 of cold acclimation in stickleback livers but CS activity remained higher compared to warm-acclimated fish throughout the remainder of the cold acclimation period. Similar results were found in the livers of cold-acclimated eelpout; the mRNA levels of CS increased on day 4 of cold acclimation and decreased on day 7, yet the maximal activity of CS activity did not become significantly elevated until day 9 and remained elevated throughout the

remainder of 25-day cold-acclimation period (44). Together, these results suggest that early increases in CS activity are driven by increases in CS transcript but long term changes in CS activity during cold acclimation are regulated by post-transcriptional mechanisms. One possibility is that a decrease in the turnover rate of CS protein may maintain its activity in the cold. The concentration of cytochrome c, a component of the mitochondrial electron transport chain, was increased in green sunfish (*Lepomis cyanellus*) in response to cold acclimation, but not because of an increase in protein synthesis. Rather, the rate of cytochrome c synthesis was depressed at cold temperature, but its degradation rate was reduced to a greater extent, resulting in a net increase in protein concentration (67). Alternatively, the activity of citrate synthase may be regulated by post-translational modifications such as methylation or phosphorylation (2, 25).

4.3 Regulation of aerobic metabolic remodeling.

Our results indicate that oxidative muscle and liver respond differently to cold acclimation. The magnitude of changes in aerobic metabolic enzymes and the time frame within which these changes occur, differed between the two tissues. This is consistent with previous studies and is not surprising given the differing metabolic functions of liver and muscle (65). Nevertheless, these results suggest differences in the molecular pathways governing metabolic remodeling between liver and oxidative muscle.

The expression of many genes central to mitochondrial function are regulated by the transcription factors NRF-1 and NRF-2 (34). NRFs *trans*-activate genes involved in oxidative phosphorylation, mtDNA transcription and replication, heme biosynthesis and protein import and assembly (34). We found that transcript levels of NRF-1 increased in response to cold acclimation in both liver and oxidative muscle. Transcript levels of NRF-1 became significantly elevated after 9 weeks at 8°C in oxidative muscle and on day 2 of cold acclimation in liver. The increase in NRF-1 in both tissues coincided with an increase in CS mRNA levels. In oxidative muscle, it also coincided with an increase in COXIV mRNA levels. Similarly, a previous study in goldfish found significant increases in NRF-1 mRNA levels in oxidative and glycolytic skeletal muscles, heart and liver in

response to cold acclimation (41). Increases in NRF-1 mRNA were also detected in the skeletal muscle of zebrafish in response to cold acclimation and exercise (47). Thus, similar to mammalian systems, NRF-1 appears to play an important role in increasing aerobic metabolic capacity in fish.

PGC-1 co-transcriptional activators (PRC, PGC-1α and PGC-1β) are considered the master regulators of mitochondrial biogenesis because they interact with, and coordinate the activity of several transcription factors governing the expression of mitochondrial-targeted genes. They also enhance transcription by recruiting histone acetyltransferases and the Mediator complex (19, 24, 62). We did not detect a significant increase in transcript levels of PGC-1α or PGC-1β in oxidative muscle in response to cold acclimation despite an increase in mitochondrial volume density. Previous studies of cold acclimation in goldfish and zebrafish also failed to detect significant an increase in the mRNA level of PGC-1α in muscle despite increases in the maximal activity of aerobically-poised enzymes (41, 47). Our ability to detect an increase in PGC-1α may have been hampered by the high degree of variability in the expression of this gene. Transcript levels of PGC-1α were significantly correlated with transcript levels of NRF-1, CS, COXIV and TFAM in oxidative muscle (Fig. 7). Another possibility is that the activity or protein level of PGC-1α increased during cold acclimation. PGC-1α activity is regulated by phosphorylation by AMPK and MAPK (28), deacetlylation by sirtuin 1 (17), and arginine methylation by protein arginine methyltransferase 1 (73).

The transcript level of PGC-1β increased on the third day of cold acclimation in liver tissue. This corresponded with an increase in NRF-1 and CS mRNA levels. Transcript levels of PGC-1β were significantly correlated with the expression of NRF-1, TFAM, CS, COXIII and COXIV in liver (Fig. 7). Similarly, there was a robust increase in PGC-1β, but not PGC-1α mRNA levels in livers of goldfish in response to cold acclimation, which corresponded with a significant increase in mRNA levels of CS (41). These results suggest that PGC-1β may play a more prominent role than PGC-1α in regulating aerobic metabolic remodeling in liver tissue during cold acclimation in fish.

PGC-1α						
0.64† / 0.74†	PGC-1β					
0.35* / 0.30*	0.12 / 0.34*	NRF-1				
0.44† / 0.38*	0.48† / 0.42*	0.47† / 0.54†	TFAM			
0.59† / 0.76†	0.18 / 0.78†	0.41* / 0.30*	0.46† / 0.39*	CS		
0.34* / 0.69†	0.22 / 0.54†	0.45† / 0.04	0.58† / 0.24	0.76† / 0.82†	COXIV	
0.20 / 0.41*	0.00 / 0.44†	0.29* / 0.23	0.34* / 0.31*	0.36* / 0.48†	0.50† / 0.53†	COXIII

Fig. 7. Pearson's product moment correlation coefficients. Correlations between gene expression levels were estimated from Pearson's product moment correlation coefficients in oxidative muscle (unshaded) and liver (shaded). mRNA levels were pooled from fish harvested at all time points during cold- and warm-acclimation. *Indicates a significant correlation ($P < 0.05$), †Indicates a significant correlation ($P < 0.001$). CS, citrate synthase; COX, cytochrome c oxidase; PGC-1, peroxisome proliferator-activated receptor γ coactivator-1; NRF-1, nuclear respiratory factor-1; TFAM, mitochondrial transcription factor A.

TFAM is a nuclear-encoded mitochondrial transcription factor which regulates transcription and replication of the mitochondrial genome. A significant increase in the mRNA levels of TFAM was correlated with an increase in mtDNA copy number but not transcript levels of the mitochondrially-encoded gene COXIII in liver. TFAM regulates mtDNA copy number and can induce mtDNA replication independently of transcription in mammals (13). TFAM mRNA levels increased at week 1 of cold acclimation, following the initial increases in PGC-1β and NRF-1 levels of mRNA. At this time both PGC-1β and NRF-1 transcript levels were still elevated compared to warm-acclimated fish, suggesting that these proteins may induce the expression of TFAM during cold acclimation.

5. PERSPECTIVES AND SIGNIFICANCE

It is currently unknown what triggers an increase in aerobic metabolic capacity in response to cold acclimation in fish. In mammals, an elevation in aerobic metabolic capacity brought about through mitochondrial biogenesis is stimulated by a variety of signaling molecules, some induced by stress and others involved in sensing the energetic status of the cell (8, 28, 33, 39). We identified two notable differences between the response of oxidative muscle and liver to cold acclimation, which taken together suggest that the stimulus and some of the components of the signaling pathway governing cold-induced metabolic remodeling differ between the two tissues. First, while cold acclimation led to an increase in the activity of aerobically-poised enzymes in both liver and muscle, mitochondrial biogenesis only occurred in muscle. Secondly, the time frame in which aerobic metabolic capacity increased differed between the two tissues. The transcription of aerobic metabolic genes and regulators of mitochondrial biogenesis (PGC-1 and NRF-1) increased within 1 week of cold acclimation in liver but not until between weeks 4 and 9 of cold acclimation in oxidative muscle. Mitochondrial biogenesis may be postponed in muscle until mitochondrial membrane remodeling is complete so that membranes of all newly synthesized organelles do not have to be remodeled. How this information might be relayed to the nuclear genome to initiate

mitochondrial biogenesis is unknown. This type of signaling, from the mitochondria to the nucleus, is known as retrograde signaling and is mediated by several signaling molecules, including TOR, Ca^{2+}, ROS and NO, all of which stimulate mitochondrial biogenesis in mammals (4). Now that we have established the time frame in which changes in aerobic metabolism occur in liver and muscle, we can identify the stimuli that mediate these changes in response to cold acclimation. Further studies will also be required to determine how aerobic capacity increases independently of mitochondrial biogenesis in liver. Given that PGC-1β, one of the key regulators of mitochondrial biogenesis in mammals increased in response to cold acclimation in liver, other proteins positioned downstream of PGC-1β likely play a role in regulating organelle proliferation.

6. ACKNOWLEDGEMENTS

We thank Kelly Edwards at the University of Maine microcopy laboratory for assistance with sample preparation for transmission electron microscopy. Electron microscopy was carried out at the Advanced Instrumentation Laboratory at UAF. Thanks to Dr. Rosemarie Plaetke for assistance with statistics and Irina Müller for technical support.

7. GRANTS

This work was supported by National Science Foundation grant IOS-0643857 to K.M.OB. Additional support was provided to J.I.O. from the Alfred P. Sloan Foundation and Alaska INBRE program.

8. DISCLOSURES

No conflicts of interest, financial or otherwise, are declared by the authors.

9. REFERENCES

1. **Battersby BJ and Moyes CD.** Influence of acclimation temperature on mitochondrial DNA, RNA, and enzymes in skeletal muscle. *Am J Physiol* 275: R905-912, 1998.

2. **Bloxham DP, Parmelee DC, Kumar S, Wade RD, Ericsson LH, Neurath H, Walsh KA, and Titani K.** Primary structure of porcine heart citrate synthase. *Proc Natl Acad Sci U S A* 78: 5381-5385, 1981.

3. **Brunner AM, Yakovlev IA, and Strauss SH.** Validating internal controls for quantitative plant gene expression studies. *BMC Plant Biol* 4: 14, 2004.

4. **Butow RA and Avadhani NG.** Mitochondrial signaling: the retrograde response. *Mol Cell* 14: 1-15, 2004.

5. **Campbell CM and Davies JS.** Temperature acclimation in the teleost, Blennius pholis: changes in enzyme activity and cell structure. *Comp Biochem Physiol* 61B: 165-167, 1978.

6. **Clay Montier LL, Deng JJ, and Bai Y.** Number matters: control of mammalian mitochondrial DNA copy number. *J Genet Genomics* 36: 125-131, 2009.

7. **Cruz-Orive LM and Weibel ER.** Sampling designs for stereology. *J Microsc* 122: 235-257, 1981.

8. **Cunningham JT, Rodgers JT, Arlow DH, Vazquez F, Mootha VK, and Puigserver P.** mTOR controls mitochondrial oxidative function through a YY1-PGC-1alpha transcriptional complex. *Nature* 450: 736-740, 2007.

9. **de Kok JB, Roelofs RW, Giesendorf BA, Pennings JL, Waas ET, Feuth T, Swinkels DW, and Span PN.** Normalization of gene expression measurements in tumor tissues: comparison of 13 endogenous control genes. *Lab Invest* 85: 154-159, 2005.

10. **Desaulniers N, Moerland TS, and Sidell BD.** High lipid content enhances the rate of oxygen diffusion through fish skeletal muscle. *Am J Physiol* 271: R42-47, 1996.

11. **Edwards K, Logan J, and Saunders N.** *Real-Time PCR: An Essential Guide*. London: Horizon Bioscience, 2004.

12. **Egginton S and Sidell BD.** Thermal acclimation induces adaptive changes in subcellular structure of fish skeletal muscle. *Am J Physiol* 256: R1-9, 1989.

13. **Ekstrand MI, Falkenberg M, Rantanen A, Park CB, Gaspari M, Hultenby K, Rustin P, Gustafsson CM, and Larsson NG.** Mitochondrial transcription factor A regulates mtDNA copy number in mammals. *Hum Mol Genet* 13: 935-944, 2004.

14. **Falkenberg M, Larsson NG, and Gustafsson CM.** DNA replication and transcription in mammalian mitochondria. *Annu Rev Biochem* 76: 679-699, 2007.

15. **Fangue NA, Richards JG, and Schulte PM.** Do mitochondrial properties explain intraspecific variation in thermal tolerance? *J Exp Biol* 212: 514-522, 2009.

16. **Frick NT, Bystriansky JS, Ip YK, Chew SF, and Ballantyne JS.** Cytochrome c oxidase is regulated by modulations in protein expression and mitochondrial membrane phospholipid composition in estivating African lungfish. *Am J Physiol Regul Integr Comp Physiol*, 2009.

17. **Gerhart-Hines Z, Rodgers JT, Bare O, Lerin C, Kim SH, Mostoslavsky R, Alt FW, Wu Z, and Puigserver P.** Metabolic control of muscle mitochondrial function and fatty acid oxidation through SIRT1/PGC-1alpha. *EMBO J* 26: 1913-1923, 2007.

18. **Grim JM, Miles DR, and Crockett EL.** Temperature acclimation alters oxidative capacities and composition of membrane lipids without influencing activities of enzymatic antioxidants or susceptibility to lipid peroxidation in fish muscle. *J Exp Biol* 213: 445-452, 2010.

19. **Handschin C and Spiegelman BM.** Peroxisome proliferator-activated receptor gamma coactivator 1 coactivators, energy homeostasis, and metabolism. *Endocr Rev* 27: 728-735, 2006.

20. **Hazel JR.** Thermal adaptation in biological membranes: is homeoviscous adaptation the explanation? *Annu Rev Physiol* 57: 19-42, 1995.

21. **Hazel JR and Landrey SR.** Time course of thermal adaptation in plasma membranes of trout kidney. I. Headgroup composition. *Am J Physiol* 255: R622-627, 1988.

22. **Helling S, Vogt S, Rhiel A, Ramzan R, Wen L, Marcus K, and Kadenbach B.** Phosphorylation and kinetics of mammalian cytochrome c oxidase. *Mol Cell Proteomics* 7: 1714-1724, 2008.

23. **Hochachka PW and Somero GN.** *Biochemical Adaptation: Mechanism and process in physiological evolution*. Oxford: Oxford University Press, 2002.

24. **Hock MB and Kralli A.** Transcriptional control of mitochondrial biogenesis and function. *Annu Rev Physiol* 71: 177-203, 2009.

25. **Hopper RK, Carroll S, Aponte AM, Johnson DT, French S, Shen RF, Witzmann FA, Harris RA, and Balaban RS.** Mitochondrial matrix phosphoproteome: effect of extra mitochondrial calcium. *Biochemistry* 45: 2524-2536, 2006.

26. **Hori A, Yoshida M, Shibata T, and Ling F.** Reactive oxygen species regulate DNA copy number in isolated yeast mitochondria by triggering recombination-mediated replication. *Nucleic Acids Res* 37: 749-761, 2009.

27. **Ibarz A, Martin-Perez M, Blasco J, Bellido D, de Oliveira E, and Fernandez-Borras J.** Gilthead sea bream liver proteome altered at low temperatures by oxidative stress. *Proteomics*, 2010.

28. **Jager S, Handschin C, St-Pierre J, and Spiegelman BM.** AMP-activated protein kinase (AMPK) action in skeletal muscle via direct phosphorylation of PGC-1alpha. *Proc Natl Acad Sci U S A* 104: 12017-12022, 2007.

29. **Jankowsky D, Hotopp W, and Seibert H.** Influence of thermal acclimation on glucose production and ketogenesis in isolated eel hepatocytes. *Am J Physiol* 246: R471-478, 1984.

30. **Johnston IA.** Capillarisation, oxygen diffusion distances and mitochondrial content of carp muscles following acclimation to summer and winter temperatures. *Cell Tissue Res* 222: 325-337, 1982.

31. **Johnston IA and Maitland B.** Temperature acclimation in crucian carp, Carassius carassius L., morphometric analyses of muscle fibre ultrastructure. *J Fish Biol* 17: 113-125, 1980.

32. **Kammer AR, Orczewska JI, and O'Brien KM.** Oxidative Stress is transient and tissue specific during cold acclimation of threespine stickleback. *J Exp Biol 214*: 1248-1256, 2011.

33. **Kang C, O'Moore KM, Dickman JR, and Ji LL.** Exercise activation of muscle peroxisome proliferator-activated receptor-gamma coactivator-1alpha signaling is redox sensitive. *Free Radic Biol Med* 47: 1394-1400, 2009.

34. **Kelly DP and Scarpulla RC.** Transcriptional regulatory circuits controlling mitochondrial biogenesis and function. *Genes Dev* 18: 357-368, 2004.

35. **Khalimonchuk O and Rodel G.** Biogenesis of cytochrome c oxidase. *Mitochondrion* 5: 363-388, 2005.

36. **Kleckner NW and Sidell BD.** Comparison of maximal activities of enzymes from tissues of thermally acclimated and naturally acclimatized chain pickerel (Esox niger). *Physiol Zool* 58: 18-28, 1985.

37. **Klingenspor M, Ivemeyer M, Wiesinger H, Haas K, Heldmaier G, and Wiesner RJ.** Biogenesis of thermogenic mitochondria in brown adipose tissue of Djungarian hamsters during cold adaptation. *Biochem J* 316 (Pt 2): 607-613, 1996.

38. **Kraffe E, Marty Y, and Guderley H.** Changes in mitochondrial oxidative capacities during thermal acclimation of rainbow trout Oncorhynchus mykiss: roles of membrane proteins, phospholipids and their fatty acid compositions. *J Exp Biol* 210: 149-165, 2007.

39. **Lagouge M, Argmann C, Gerhart-Hines Z, Meziane H, Lerin C, Daussin F, Messadeq N, Milne J, Lambert P, Elliott P, Geny B, Laakso M, Puigserver P, and Auwerx J.** Resveratrol improves mitochondrial function and protects against metabolic disease by activating SIRT1 and PGC-1alpha. *Cell* 127: 1109-1122, 2006.

40. **Leary SC, Battersby BJ, and Moyes CD.** Inter-tissue differences in mitochondrial enzyme activity, RNA and DNA in rainbow trout (Oncorhynchus mykiss). *J Exp Biol* 201 (Pt 24): 3377-3384, 1998.

41. **Lemoine CM, Genge CE, and Moyes CD.** Role of the PGC-1 family in the metabolic adaptation of goldfish to diet and temperature. *J Exp Biol* 211: 1448-1455, 2008.

42. **Lin J, Puigserver P, Donovan J, Tarr P, and Spiegelman BM.** Peroxisome proliferator-activated receptor gamma coactivator 1beta (PGC-1beta), a novel PGC-1-related transcription coactivator associated with host cell factor. *J Biol Chem* 277: 1645-1648, 2002.

43. **Lucassen M, Koschnick N, Eckerle LG, and Portner HO.** Mitochondrial mechanisms of cold adaptation in cod (Gadus morhua L.) populations from different climatic zones. *J Exp Biol* 209: 2462-2471, 2006.

44. **Lucassen M, Schmidt A, Eckerle LG, and Portner HO.** Mitochondrial proliferation in the permanent vs. temporary cold: enzyme activities and mRNA levels in Antarctic and temperate zoarcid fish. *Am J Physiol Regul Integr Comp Physiol* 285: R1410-1420, 2003.

45. **Martin I, Vinas O, Mampel T, Iglesias R, and Villarroya F.** Effects of cold environment on mitochondrial genome expression in the rat: evidence for a tissue-specific increase in the liver, independent of changes in mitochondrial gene abundance. *Biochem J* 296 (Pt 1): 231-234, 1993.

46. **Mathews CK and VanHolde KE.** *Biochemistry*. New York: Benjamin Cummings, 1996.

47. **McClelland GB, Craig PM, Dhekney K, and Dipardo S.** Temperature- and exercise-induced gene expression and metabolic enzyme changes in skeletal muscle of adult zebrafish (Danio rerio). *J Physiol* 577: 739-751, 2006.

48. **Moerland TS.** Temperature: enzyme and organelle. In: *Biochemistry and molecular biology of fishes* edited by Mommsen Ha: Elsevier Science, 1995.

49. **Moraes CT.** What regulates mitochondrial DNA copy number in animal cells? *Trends Genet* 17: 199-205, 2001.

50. **Moreno-Loshuertos R, Acin-Perez R, Fernandez-Silva P, Movilla N, Perez-Martos A, Rodriguez de Cordoba S, Gallardo ME, and Enriquez JA.** Differences in reactive oxygen species production explain the phenotypes associated with common mouse mitochondrial DNA variants. *Nat Genet* 38: 1261-1268, 2006.

51. **Nisoli E, Clementi E, Paolucci C, Cozzi V, Tonello C, Sciorati C, Bracale R, Valerio A, Francolini M, Moncada S, and Carruba MO.** Mitochondrial biogenesis in mammals: the role of endogenous nitric oxide. *Science* 299: 896-899, 2003.

52. **O'Brien KM and Sidell BD.** The interplay among cardiac ultrastructure, metabolism and the expression of oxygen-binding proteins in Antarctic fishes. *J Exp Biol* 203: 1287-1297, 2000.

53. **Olsvik PA, Lie KK, Jordal AE, Nilsen TO, and Hordvik I.** Evaluation of potential reference genes in real-time RT-PCR studies of Atlantic salmon. *BMC Mol Biol* 6: 21, 2005.

54. **Paradies G, Petrosillo G, Pistolese M, Di Venosa N, Serena D, and Ruggiero FM.** Lipid peroxidation and alterations to oxidative metabolism in mitochondria isolated from rat heart subjected to ischemia and reperfusion. *Free Radic Biol Med* 27: 42-50, 1999.

55. **Pfaffl MW, Tichopad A, Prgomet C, and Neuvians TP.** Determination of stable housekeeping genes, differentially regulated target genes and sample integrity: BestKeeper--Excel-based tool using pair-wise correlations. *Biotechnol Lett* 26: 509-515, 2004.

56. **Podrabsky JE and Somero GN.** Changes in gene expression associated with acclimation to constant temperatures and fluctuating daily temperatures in an annual killifish Austrofundulus limnaeus. *J Exp Biol* 207: 2237-2254, 2004.

57. **Puigserver P, Wu Z, Park CW, Graves R, Wright M, and Spiegelman BM.** A cold-inducible coactivator of nuclear receptors linked to adaptive thermogenesis. *Cell* 92: 829-839, 1998.

58. **Puntel RL, Nogueira CW, and Rocha JB.** Krebs cycle intermediates modulate thiobarbituric acid reactive species (TBARS) production in rat brain in vitro. *Neurochem Res* 30: 225-235, 2005.

59. **Savagner F, Mirebeau D, Jacques C, Guyetant S, Morgan C, Franc B, Reynier P, and Malthiery Y.** PGC-1-related coactivator and targets are upregulated in thyroid oncocytoma. *Biochem Biophys Res Commun* 310: 779-784, 2003.

60. **Scarpulla RC.** Nuclear control of respiratory chain expression by nuclear respiratory factors and PGC-1-related coactivator. *Ann N Y Acad Sci* 1147: 321-334, 2008.

61. **Scarpulla RC.** Nuclear control of respiratory chain expression in mammalian cells. *J Bioenerg Biomembr* 29: 109-119, 1997.

62. **Scarpulla RC.** Transcriptional paradigms in Mammalian mitochondrial biogenesis and function. *Physiol Rev* 88: 611-638, 2008.

63. **Scheffler IE.** *Mitochondria*. New York: Wiley, 1999.

64. **Sedlak E and Robinson NC.** Phospholipase A(2) digestion of cardiolipin bound to bovine cytochrome c oxidase alters both activity and quaternary structure. *Biochemistry* 38: 14966-14972, 1999.

65. **Shaklee JB, Christiansen JA, Sidell BD, Prosser CL, and Whitt GS.** Molecular aspects of temperature acclimation in fish: Contributions of changes in enzyme activities and isozyme patterns to metabolic reorganization in the green sunfish. *J Exp Zool* 201: 1-20, 1977.

66. **Sidell BD.** Intracellular oxygen diffusion: the roles of myoglobin and lipid at cold body temperature. *Journal of Experimental Biology* 201: 1118-1127, 1998.

67. **Sidell BD.** Turnover of cytochrome c in skeletal muscle of green sunfish (Lepomis cyanellus R.) during thermal acclimation. *J Exp Zool* 199: 233-250, 1977.

68. **Sogl B, Gellissen G, and Wiesner RJ.** Biogenesis of giant mitochondria during insect flight muscle development in the locust, Locusta migratoria (L.). Transcription, translation and copy number of mitochondrial DNA. *Eur J Biochem* 267: 11-17, 2000.

69. **Somero GN.** Adaptation of enzymes to temperature: searching for basic "strategies". *Comp Biochem Physiol B Biochem Mol Biol* 139: 321-333, 2004.

70. **Stone BB and Sidell BD.** Metabolic responses of striped bass (Morone saxatilis) to temperature acclimation. I. Alterations in carbon sources for hepatic energy metabolism. *J Exp Zool* 218: 371-379, 1981.

71. **Subczynski WK, Widomska J, and Feix JB.** Physical properties of lipid bilayers from EPR spin labeling and their influence on chemical reactions in a membrane environment. *Free Radic Biol Med* 46: 707-718, 2009.

72. **Suliman HB, Carraway MS, Tatro LG, and Piantadosi CA.** A new activating role for CO in cardiac mitochondrial biogenesis. *J Cell Sci* 120: 299-308, 2007.

73. **Teyssier C, Ma H, Emter R, Kralli A, and Stallcup MR.** Activation of nuclear receptor coactivator PGC-1alpha by arginine methylation. *Genes Dev* 19: 1466-1473, 2005.

74. **Trueman RJ, Tiku PE, Caddick MX, and Cossins AR.** Thermal thresholds of lipid restructuring and delta(9)-desaturase expression in the liver of carp (Cyprinus carpio L.). *J Exp Biol* 203: 641-650, 2000.

75. **Tyler S and Sidell BD.** Changes in mitochondrial distribution and diffusion distances in muscle of goldfish upon acclimation to warm and cold temperatures. *Journal of Experimental Zoology* 232: 1-9, 1984.

76. **Vezina D and Guderley H.** Anatomic and enzymatic responses of the three-spined stickleback, *Gasterosteus aculeatus* to thermal acclimation. *The Journal of Experimental Zoology* 258: 277-287, 1991.

77. **Weibel ER.** *Stereological Methods*. New York: Academic Press, 1979.

78. **Weibel ER, Kistler GS, and Scherle WF.** Practical stereological methods for morphometric cytology. *J Cell Biol* 30: 23-38, 1966.

79. **Wharton DC and Tzagoloff A.** Cytochrome oxidase from beef heart mitochondria. *Methods in Enzymology* 10: 245-250, 1967.

80. **Wodtke E.** Temperature adaptation of biological membranes. Compensation of the molar activity of cytochrome c oxidase in the mitochondrial energy-transducing membrane during thermal acclimation of the carp (Cyprinus carpio L.). *Biochim Biophys Acta* 640: 710-720, 1981.

81. **Wooten RJ.** *A functional biology of sticklebacks*. Berkeley and Los Angeles: University of California Press, 1984.

82. **Wu H, Kanatous SB, Thurmond FA, Gallardo T, Isotani E, Bassel-Duby R, and Williams RS.** Regulation of mitochondrial biogenesis in skeletal muscle by CaMK. *Science* 296: 349-352, 2002.

APPENDIX A: GLYCOLYTIC MUSCLE

A.1 Introduction

Aerobic metabolic capacity increases in muscle in response to cold acclimation in many species of fish (2, 3, 8, 9, 22, 23). The maximal activity of the aerobically-poised enzymes citrate synthase (CS) and cytochrome c oxidase (COX) were elevated in both the oxidative and glycolytic muscles of common carp, rainbow trout, and chain pickerel exposed to cold temperature (1, 10, 12). Although the response of the oxidative and glycolytic muscles has been well documented in many species of fish, previous studies have analyzed only the metabolic status of fishes at the end points of warm and cold acclimation, so it is unclear if the time frame for metabolic remodeling is similar between these two muscle types. Furthermore, few studies have examined the transcriptional regulatory factors responsible for stimulating metabolic remodeling in muscle, so it is unknown if changes in aerobic capacity are regulated similarly between oxidative and glycolytic muscles.

Oxidative and glycolytic muscles differ in their dominant metabolic pathways as well as in quantity of mitochondria, concentration of myoglobin, capillary density and glycogen content (3, 18). In the oxidative muscle fibers of striped bass, the percentage of cell volume displaced by mitochondria was found to be as high as 45%, whereas in glycolytic muscle, mitochondria occupied only 4% of the cell volume (3). Not only do mitochondrial volume densities differ between muscle types, but the mean cross-sectional area of mitochondria also differs. In striped bass, the cross sectional area of individual oxidative-muscle mitochondria was 1.4-fold larger than those in glycolytic muscle (3). Not surprisingly, the capillary density of oxidative muscle, which relies on aerobic metabolism, is 7 times greater than the density of capillaries in glycolytic muscle (3). Additionally, the maximal activity of CS was 5.1-fold higher in oxidative muscle compared to glycolytic muscle in rainbow trout (15).

The differences in physiology and biochemistry between oxidative and glycolytic muscles suggest their response to cold acclimation and regulatory factors mediating these changes may also differ. To address this question, threespine stickleback were captured and held at 20°C for 12 weeks and either cold acclimated to 8°C or maintained at 20°C for an additional 9 weeks. Mitochondrial DNA copy number and the maximal activity of CS and COX was

quantified in the glycolytic muscle of cold- and warm- acclimated animals. Additionally, mRNA levels of the aerobic metabolic genes citrate synthase (CS) and cytochrome c oxidase subunits III and IV (COXIII and COXIV), as well as known regulators of mitochondrial biogenesis, peroxisome proliferator-activated receptor-gamma coactivators-1α and -1β (PGC-1α and PGC-1β), nuclear respiratory factor-1 (NRF-1), and mitochondrial transcription factor-A (TFAM) were quantified throughout the time course of cold acclimation.

A.2 Results

A.2.1 Time course for metabolic remodeling in response to cold acclimation

Mitochondrial DNA copy number did not significantly increase in response to cold acclimation in glycolytic muscle (Fig. A.1).

The aerobic metabolic capacity of glycolytic muscle was assessed throughout the time course of cold acclimation by measuring the maximal activity of CS and COX at a common temperature of 10°C and 14°C, respectively. The maximal activity of COX was significantly higher in animals maintained at 8°C for 9 weeks compared to those held at 20°C for 9 weeks. At this point, the maximal activity of COX had increased 1.5-fold compared to fish at 20°C for 9 weeks ($P < 0.05$) (Fig. A.2). The maximal activity of CS did not significantly increase in glycolytic muscle when compared across all time points using a non-parametric Kruskall Wallis statistical test. However, when the maximal activity of CS was compared between animals at 8°C and 20°C after 9 weeks using a student's t-test, CS activity was significantly higher in cold acclimated animals ($P < 0.05$) (Fig. A.2).

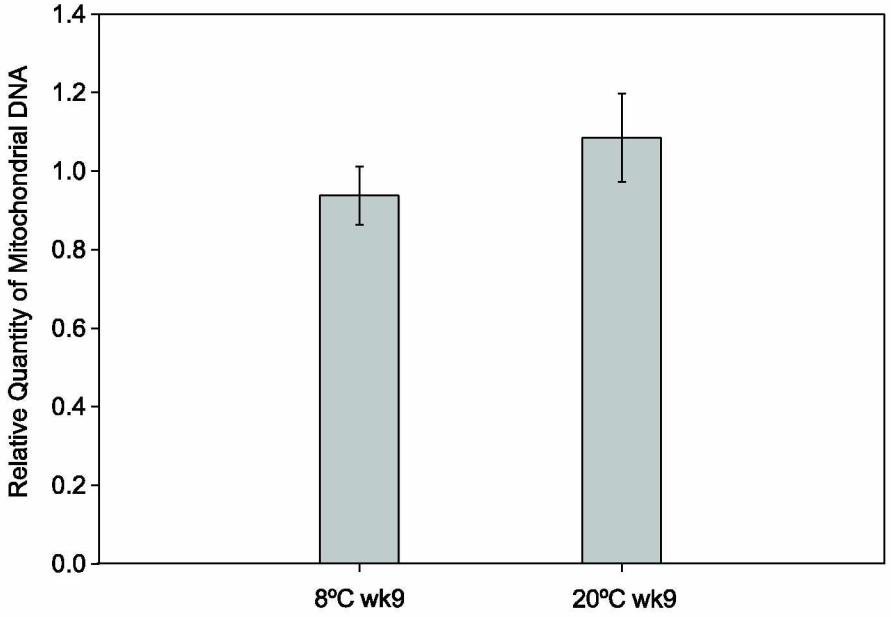

Fig. A.1. Changes in mitochondrial DNA copy number in glycolytic muscle. The ratio of mtDNA-to-nDNA was quantified by measuring levels of the mitochondrially-encoded gene COXIII and the nuclear-encoded gene CYC in animals held at 8°C for 9 weeks and 20°C for 9 weeks using qRT-PCR. (N=6). Values are presented as means ± SE.

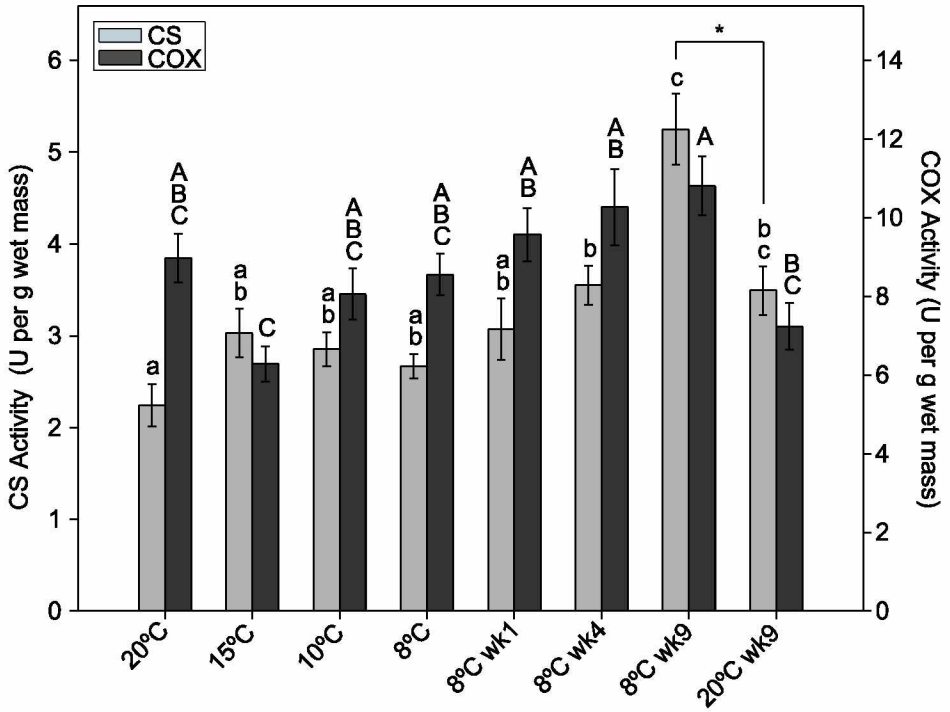

Fig. A.2. Maximal activity of aerobic metabolic enzymes in glycolytic muscle. The maximal activity of CS and COX was measured at a common temperature during cold acclimation. Values are presented as means ± SE (N=4-6) Different letters within a series denote significant differences among warm- and cold-acclimated fish ($P < 0.05$). *Indicates a significant difference between animals at 8°C and 20°C after 9 weeks using a student's t-test. CS, citrate synthase; COX, cytochrome c oxidase.

A.2.2 Identification of a stable housekeeping gene

The stability of four potential housekeeping genes (18S, ACTB, TBP, EF-1α) was analyzed in warm- (20°C and 20°C week 9) and cold- acclimated fish (8°C week 9) using *Bestkeeper*©. The standard deviation of ACTB expression was greater than 1.0 between samples and was therefore excluded from the remainder of the analysis. Measurements of 18S, TBP, and EF-1α transcript levels all had a standard deviation less than 1.0. However; only TBP and EF-1α were significantly correlated with the *Bestkeeper Index* (Table A.1). The mRNA levels of TBP were significantly different between warm- and cold-acclimated fish in oxidative muscle ($P < 0.05$). As a result, TBP was excluded as a potential HKG and EF-1α was used for normalizing the expression of target genes (Table A.1).

A.2.3 Changes in the expression of aerobic metabolic genes in response to cold acclimation

CS mRNA levels were significantly higher in animals after 9 weeks at 8°C compared to animals at 20°C for 9 weeks ($P < 0.05$) (Fig. A.3A). The increase in transcript levels of CS coincided with an increase in CS activity (Fig. A.2). Transcript levels of two subunits of COX, nuclear-encoded COXIV and mitochondrially-encoded COXIII, were measured during cold acclimation. mRNA levels of COXIV were significantly lower in animals at 8°C after 1 week compared to those at 20°C (Fig. A.3B). After 9 weeks at 8°C the relative mRNA levels of COXIV significantly increased compared to animals after 1 week at 8°C and were equivalent to mRNA levels in animals held at 20°C for 9 weeks ($P < 0.05$) (Fig. A.3B). There was no significant change in the expression of COXIII with cold acclimation ($P > 0.05$) (Fig. A.3C).

Table A.1. Housekeeping gene analysis for glycolytic muscle using Bestkeeper©

Gene	SD	*r*	*P* Value for *r*	*F*-Value for ANOVA
18S	0.54	-0.104	0.587	0.003
ACTB	1.18	0.343	0.093	0.0004
EF-1α	0.71	0.55	0.005	0.4016
TBP	0.91	0.781	0.001	< 0.0001

SD, Standard deviation of critical threshold (Ct) values; r, Pearson correlation coefficient comparing Ct values of selected housekeeping genes with the *Bestkeeper Index*. (N=8-10).

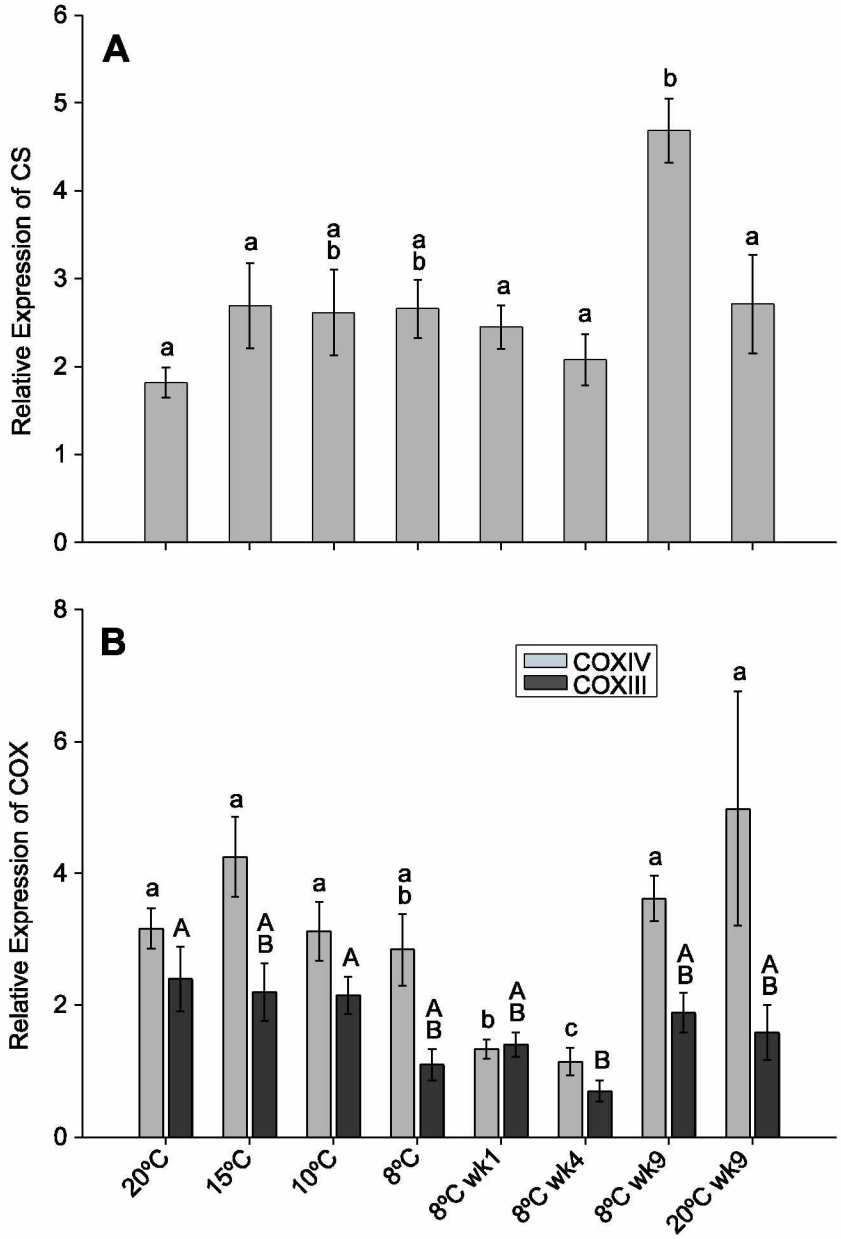

Fig. A.3. Transcript levels of aerobic metabolic genes in glycolytic muscle. Transcript levels of CS (A), and two subunits of COX (B), nuclear-encoded COXIV and mitochondrially-encoded COXIII, were quantified using qRT-PCR. mRNA levels were normalized to EF-1α. Values are presented as means ± SE (N=5-8). Different letters within a series denote significant differences among cold- and warm -acclimated fish ($P < 0.05$). CS, citrate synthase; COX, cytochrome c oxidase.

A.2.4 Changes in the expression of genes involved in regulating aerobic remodeling in response to cold acclimation

The relative expression of PGC-1α was significantly elevated on the second and third day of cold acclimation, at 10°C and 8°C respectively, when compared to animals at 20°C ($P < 0.05$) (Fig. A.4A). After 1 week at 8°C the expression of PGC-1α was no longer significantly different from control animals at 20°C ($P < 0.05$) (Fig. A.4A). PGC-1β transcript levels significantly increased on day 2 of cold acclimation at 10°C compared to animals at 20°C ($P < 0.05$) (Fig. A.4A). The relative expression of PGC-1β was significantly lower in animals after 4 weeks at 8°C compared to animals at both control groups 20°C ($P < 0.05$) (Fig. A.4A). The mRNA level of NRF-1 increased at 15°C and remained elevated in animals at 10°C compared to fish at 20°C (Fig. A.4B). By day 3 at 8°C the expression of NRF-1 was no longer significantly different between warm- and cold-acclimated animals ($P < 0.05$) (Fig. A.4B). The expression of TFAM significantly decreased after 1 week at 8°C compared to animals held at 20°C ($P < 0.05$) (Fig. A.4C). Transcript levels of TFAM remained depressed after 4 weeks at 8°C compared to both control groups at 20°C ($P < 0.05$) (Fig. A.4C). After 9 weeks at 8°C the transcript levels of TFAM were no longer significantly different than animals held at 20°C for 9 weeks ($P < 0.05$) (Fig. A.4C).

A.3 Discussion

A.3.1 Metabolic remodeling in response to cold acclimation in the glycolytic muscle

The ratio of mtDNA-to-nDNA did not increase in the glycolytic muscle in response to cold acclimation, which is consistent with studies in the glycolytic muscle of rainbow trout acclimated to 4°C compared to animals held at 18°C (1). Similarly, the copy number of mtDNA did not change in the oxidative muscle of stickleback in response to cold acclimation (22). As shown previously, mtDNA copy numbers do not appear to be the main determinants of mitochondrial content in cold-acclimated fish so it

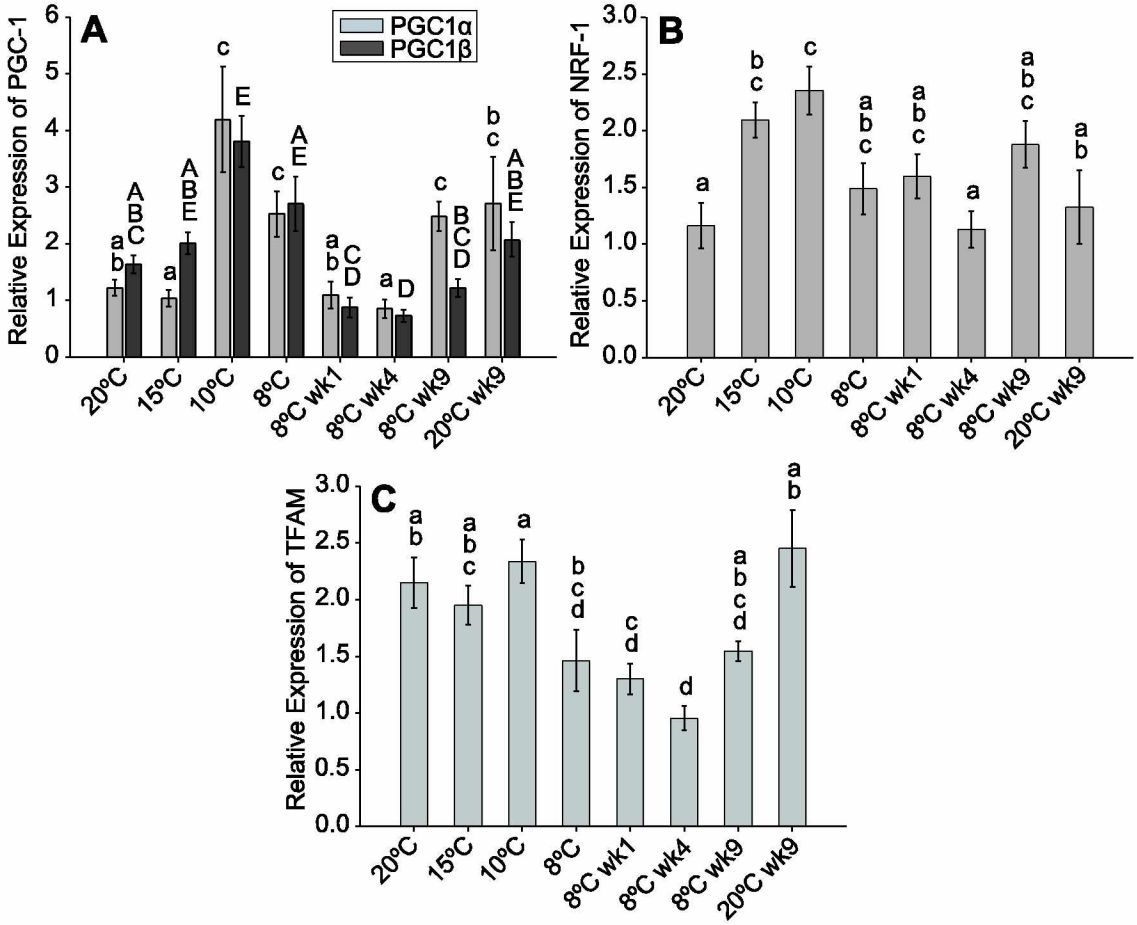

Fig. A.4. Transcript levels of genes involved in regulating aerobic metabolic remodeling in glycolytic muscle. mRNA expression of PGC-1α and PGC-1β (A), NRF-1 (B) and TFAM (C) were quantified using qRT-PCR. Transcript levels were normalized to EF-1α. Values are presented as means ± SE (N=6-8). Different letters within a series denote significant differences among cold- and warm-acclimated fish ($P < 0.05$). PGC-1, peroxisome proliferator-activated receptor γ coactivator-1; NRF-1, nuclear respiratory factor-1; TFAM, mitochondrial transcription factor A.

is unclear whether mitochondrial density increased in glycolytic muscle in response to cold acclimation (22).

The maximal activity of both CS and COX increased in glycolytic muscle after 9 weeks at 8°C independent of an increase in mtDNA copy number. Similarly, cold acclimation of rainbow trout (*Oncorhynchus mykiss*) led to an increase in CS and COX activity but not mtDNA copy number in glycolytic or oxidative skeletal muscle (1). In rainbow trout, CS activity was higher in oxidative muscle than glycolytic muscle, reflecting differences in mitochondrial density but the copy number of mtDNA was similar between the two muscle types (15). As previously described, measurements of aerobic metabolic enzymes or mtDNA alone should be used with caution to draw conclusions about changes in mitochondrial density in fishes during cold acclimation (22).

CS activity increased in glycolytic muscle after 9 weeks at 8°C which is consistent with changes seen in the oxidative muscle of threespine stickleback during cold acclimation (22). Notably, the activity of COX was found to be significantly elevated in the oxidative muscle as early as the third day of cold acclimation at 8°C, whereas the glycolytic muscle required 9 weeks at 8°C for an increase in COX activity to be observed (22). The increase in aerobic metabolic capacity in glycolytic muscle is consistent with previous studies of cold acclimation in goldfish, rainbow trout, carp, and adult zebrafish (1, 4, 10, 16, 19). However, in previous studies of cold-acclimated threespine stickleback, CS was elevated in glycolytic muscle in the absence of an increase in the activity of COX after 11 weeks of cold acclimation (4, 5). It is unclear why this discrepancy in the activity of COX occurs in threespine stickleback during cold acclimation however differences in populations of stickleback may play a role. The present study harvest animals from Kashwitna Lake, AK 12 weeks prior to the cold acclimation treatment whereas the study by Guderley et al (2001) characterized cold acclimation in sticklebacks reared in the laboratory.

The Q_{10} temperature coefficient measures the effect of a 10°C change in temperature on the rate of a chemical reaction. As a result of the Q_{10} effect, decreases in

body temperature result in a decrease in enzyme activity, which ectotherms must compensate for to maintain metabolic rate and energy production. Previous studies in threespine stickleback determined that the Q_{10} for CS was 1.55 and 1.51 for COX (5). In the present study, the maximal activity of both CS and COX increased 1.5-fold in glycolytic muscle, suggesting that the observed increase in aerobic metabolic capacity may compensate for the depressive effects of cold temperature on the catalytic rates of these enzymes *in vivo*. Additionally, the similar fold changes in the activity of CS and COX in glycolytic muscle suggest a conserved relationship between the ratio of cristae and matrix enzymes during cold acclimation.

The 1.5-fold increase in the maximal activity of CS and COX in glycolytic muscle was less than the fold-changes observed in either oxidative muscle or liver tissue of threespine stickleback in response to cold acclimation (22). In oxidative muscle, COX and CS activity 1.9-fold and 1.7-fold respectively, whereas in liver tissue, COX activity increased 1.5-fold and CS activity increased 2-fold after 9 weeks of cold acclimation (22). In glycolytic muscle, the production of ATP supply is largely dependent on glycolysis. The present study examined only the activity of aerobic metabolic enzymes because the aim of this study was to determine how mitochondrial biogenesis is regulated. However, previous studies of cold acclimation of adult zebrafish found an increase in the maximal activity of anaerobically-poised enzymes, including lactate dehydrogenase (LDH) and pyruvate kinase (PK) in glycolytic muscle (19). Furthermore, in the glycolytic muscle of gilthead seam bream, the activities of LDH and hexokinase (HK) were significantly elevated after only 1 day exposure to 10°C and PK increased after 5 days at 10°C (14). The observed early increase in the activities of LDH, PK and HK in the glycolytic muscle of fishes during cold acclimation may reflect the importance of maintaining anaerobic metabolic pathways in this tissue.

A.3.2 The molecular basis of metabolic remodeling in the glycolytic muscle

Consistent with results obtained in oxidative muscle and liver tissue, our results suggest that the activity of the aerobic metabolic enzymes CS and COX are differentially

regulated in glycolytic muscle. The maximal activity of CS and CS mRNA levels increased at week 9 of cold acclimation, suggesting transcriptional control of CS activity during cold acclimation (22). In contrast to CS, the activity of COX appears to be post-transcriptionally regulated. The maximal activity of COX increased in glycolytic muscle after 9 weeks at 8°C independently of an increase in the mRNA levels of the nuclear encoded subunit, COXIII or the mitochondrial-encoded subunit, COXIV. As previously described, COX is a multimeric protein requiring more than 20 proteins to assemble the holoenzyme suggesting alterations in any of these proteins may impact COX activity (11). Additionally, COX activity has also been shown to be influenced by phosphorylation (7) and the lipid environment (13, 24).

A.3.3 Transcriptional regulation of metabolic remodeling in the glycolytic muscle

PGC-1α and PGC-1β significantly increased in glycolytic muscle on the second day of cold acclimation at 10°C (Fig. A.4A). The increase in these co-transcriptional activators coincided with an increase in the mRNA levels of the transcriptional activator NRF-1 but not TFAM (Fig. A.4B, Fig. A.4C). An increase in the expression of NRF-1 has also been shown to be elevated in the glycolytic muscle of cold-acclimated adult zebrafish and goldfish (16, 19). In goldfish, the increase in the expression of NRF-1 in response to cold acclimation was significantly correlated with CS expression (r^2=0.54) (16). In the oxidative muscle and liver tissue of threespine stickleback, the expression of NRF-1 was also significantly correlated (r^2=0.41 and r^2=0.30, respectively) with the expression of CS during cold acclimation (22). Interestingly, the increase in mRNA levels of NRF-1 in glycolytic muscle did not coincide with increases in expression or activity of CS. Moreover, the elevations in the expression of PGC-1 and NRF-1 in the glycolytic muscle were more than 9 weeks prior to the increase in mRNA levels of CS. PGC-1 and NRF-1 play a dynamic role in mediating metabolism within the cell. Our data suggests these transcriptional regulators may mediate changes not specific to aerobic metabolism in glycolytic muscle.

The role PGC-1α, PGC-1β and NRF-1 play in the glycolytic muscle is unclear. However, the multiple roles these transcription and co-transcription factors play in cell physiology suggest several possibilities. Recent analysis of the evolution of PGC-1α structure in teleosts has identified several insertions within the NRF-1 binding domain (17). The large number of insertions in this region and rapid evolution among teleosts suggests a loss of functional interaction between PGC-1α and NRF-1 in mediating mitochondrial biogenesis (17). In contrast to NRF-1, the binding site for myocyte enhancer factor 2c (MEF2c) within PGC-1α appears to be conserved in teleosts (17). In cultured mytotubes PGC-1α was shown interact with MEF2c during the induction of the expression of insulin-responsive glucose transporter 4 (GLUT4) leading to an increase in both basal and insulin-stimulated glucose transport (20). In this regard, PGC-1α may play a role in maintaining anaerobic metabolism during cold acclimation by increasing glucose uptake.

A.3.4 Summary

Environmental changes in temperature can profoundly affect the physiology of ectothermic organisms. Temperature fluctuation at the cellular level causes changes in membrane fluidity, enzyme activity, molecular diffusion rates and ultimately, cellular energy production (6). Fishes, unlike mammals, maintain the ability to fine-tune the mitochondrial biogenic pathway allowing them to modify mitochondrial characteristics to meet specific needs of each tissue (21). This allows the cell to distinguish between, and respond specifically to, the type of stress encountered during cold acclimation.

Our results provide several new insights regarding the molecular basis of metabolic remodeling in response to cold acclimation in threespine stickleback. Whereas the maximal activity of aerobic metabolic enzymes increased in all tissues investigated, the response of aerobic metabolic enzymes in glycolytic muscle occurred late in cold acclimation. Our data suggest that the increase in the expression of PGC-1 and NRF-1 in the glycolytic muscle does not coincide with an increase in aerobic metabolism but may play a role in anaerobic metabolic remodeling.

A.4 References

1. **Battersby BJ and Moyes CD.** Influence of acclimation temperature on mitochondrial DNA, RNA, and enzymes in skeletal muscle. *Am J Physiol* 275: R905-912, 1998.

2. **Egginton S and Johnston IA.** Effects of acclimation temperature on routine metabolism, muscle mitochondrial volume density and capillary supply in the elver (*Anguilla anguilla* L.). *J Thermal Biol* 9: 165-170, 1984.

3. **Egginton S and Sidell BD.** Thermal acclimation induces adaptive changes in subcellular structure of fish skeletal muscle. *Am J Physiol* 256: R1-9, 1989.

4. **Guderley H and Leroy PH.** Family origin and the response of threespine stickleback, Gasterosteus aculeatus, to thermal acclimation. *J Comp Physiol [B]* 171: 91-101, 2001.

5. **Guderley H, Leroy PH, and Gagne A.** Thermal acclimation, growth, and burst swimming of threespine stickleback: enzymatic correlates and influence of photoperiod. *Physiol Biochem Zool* 74: 66-74, 2001.

6. **Guderley H and St-Pierre J.** Going with the flow or life in the fast lane: contrasting mitochondrial responses to thermal change. *J Exp Biol* 205: 2237-2249, 2002.

7. **Helling S, Vogt S, Rhiel A, Ramzan R, Wen L, Marcus K, and Kadenbach B.** Phosphorylation and kinetics of mammalian cytochrome c oxidase. *Mol Cell Proteomics* 7: 1714-1724, 2008.

8. **Johnston IA.** Capillarisation, oxygen diffusion distances and mitochondrial content of carp muscles following acclimation to summer and winter temperatures. *Cell Tissue Res* 222: 325-337, 1982.

9. **Johnston IA and Maitland B.** Temperature acclimation in crucian carp, *Carassius carassius* L., morphometric analyses of muscle fibre ultrastructure. *Journal of Fish Biology* 17: 113-125, 1980.

10. **Johnston IA, Sidell BD, and Driedzic WR.** Force-velocity characteristics and metabolism of carp muscle fibres following temperature acclimation. *J Exp Biol* 119: 239-249, 1985.

11. **Khalimonchuk O and Rödel G.** Biogenesis of cytochrome *c* oxidase. *Mitochondrion* 5: 363-388, 2005.

12. **Kleckner NW and Sidell BD.** Comparison of maximal activities of enzymes from tissues of thermally acclimated and naturally acclimated chain pickerel (*Esox niger*). *Physiol Zool* 58: 18-28, 1985.

13. **Kraffe E, Marty Y, and Guderley H.** Changes in mitochondrial oxidative capacities during thermal acclimation of rainbow trout Oncorhynchus mykiss: roles of membrane proteins, phospholipids and their fatty acid compositions. *J Exp Biol* 210: 149-165, 2007.

14. **Kyprianou TD, Portner HO, Anestis A, Kostoglou B, Feidantsis K, and Michaelidis B.** Metabolic and molecular stress responses of gilthead seam bream Sparus aurata during exposure to low ambient temperature: an analysis of mechanisms underlying the winter syndrome. *J Comp Physiol B* 180: 1005-1018, 2010.

15. **Leary SC, Battersby BJ, and Moyes CD.** Inter-tissue differences in mitochondrial enzyme activity, RNA and DNA in rainbow trout (Oncorhynchus mykiss). *J Exp Biol* 201 (Pt 24): 3377-3384, 1998.

16. **Lemoine CM, Genge CE, and Moyes CD.** Role of the PGC-1 family in the metabolic adaptation of goldfish to diet and temperature. *J Exp Biol* 211: 1448-1455, 2008.

17. **LeMoine CM, Lougheed SC, and Moyes CD.** Modular evolution of PGC-1alpha in vertebrates. *J Mol Evol* 70: 492-505.

18. **Martinez M, Guderley H, Dutil JD, Winger PD, He P, and Walsh SJ.** Condition, prolonged swimming performance and muscle metabolic capacities of cod Gadus morhua. *J Exp Biol* 206: 503-511, 2003.

19. **McClelland GB, Craig PM, Dhekney K, and Dipardo S.** Temperature- and exercise-induced gene expression and metabolic enzyme changes in skeletal muscle of adult zebrafish (Danio rerio). *J Physiol* 577: 739-751, 2006.

20. **Michael LF, Wu Z, Cheatham RB, Puigserver P, Adelmant G, Lehman JJ, Kelly DP, and Spiegelman BM.** Restoration of insulin-sensitive glucose transporter (GLUT4) gene expression in muscle cells by the transcriptional coactivator PGC-1. *Proc Natl Acad Sci U S A* 98: 3820-3825, 2001.

21. **O'Brien KM.** Mitochondrial biogenesis in cold-bodied fishes. *J Exp Biol* 214: 275-285, 2010.

22. **Orczewska JI, Hartleben G, and O'Brien KM.** The molecular basis of aerobic metabolic remodeling differs between oxidative muscle and liver of threespine sticklebacks in response to cold acclimation. *Am J Physiol Regul Integr Comp Physiol* 299: R352-364, 2010.

23. **Tyler S and Sidell BD.** Changes in mitochondrial distribution and diffusion distances in muscle of goldfish upon acclimation to warm and cold temperatures. *Journal of Experimental Zoology* 232: 1-9, 1984.

24. **Wodtke E.** Temperature adaptation of biological membranes. Compensation of the molar activity of cytochrome c oxidase in the mitochondrial energy-transducing membrane during thermal acclimation of the carp (Cyprinus carpio L.). *Biochim Biophys Acta* 640: 710-720, 1981.

APPENDIX B: SUPPLEMENTARY DATA

B.1 Light micrographs

As described in materials and methods, semi-thin sections (0.5 – 1.5 µm) of oxidative muscle and liver tissue from animals held at 8°C and 20°C for 9 weeks were cut and stained for measuring the cross sectional area of cells. Images were captured at a final magnification of 40X for oxidative muscle and 100X for liver tissue (Fig. B.1)

B.2 Subsarcolemmal and intramyofibrillar mitochondrial densities

As described in materials and methods, oxidative pectoral adductor muscle and liver tissues were excised from 6 fish held at 8°C and 20°C for 9 weeks. Subsarcollemal and intramyofibrillar volume densities were quantified using electron microscopy and sterological methods (Table B.1).

B.3 Total RNA mg tissue^{-1} during cold acclimation

As described in materials and methods, total RNA was excised from the oxidative muscle, glycolytic muscle and liver tissue of 6-12 fish during the time course of cold acclimation. (Table B.2).

B.4 Stickleback cDNA sequences and qRT-primer design

As described in materials and methods, transcript levels of 18S, β-Actin, CS, CYC, COXIII, COXIV, EF-1α, TBP, PGC-1α, PGC-1β, NRF-1 and TFAM were measured in animals harvested during cold acclimation using quantitative real-time PCR. Gene-specific primers were designed using sequence information obtained from Ensembl (www.ensembl.org) and the software Primer Express (Applied Biosystems). For quantification of nuclear cDNA sequences, at least one primer from each pair was designed to span a splice site to ensure that genomic DNA was not amplified. In the following sequences the splice sites and location of qRT-primers used for the analysis of gene expression in threespine stickleback are given (Fig. B1-B10).

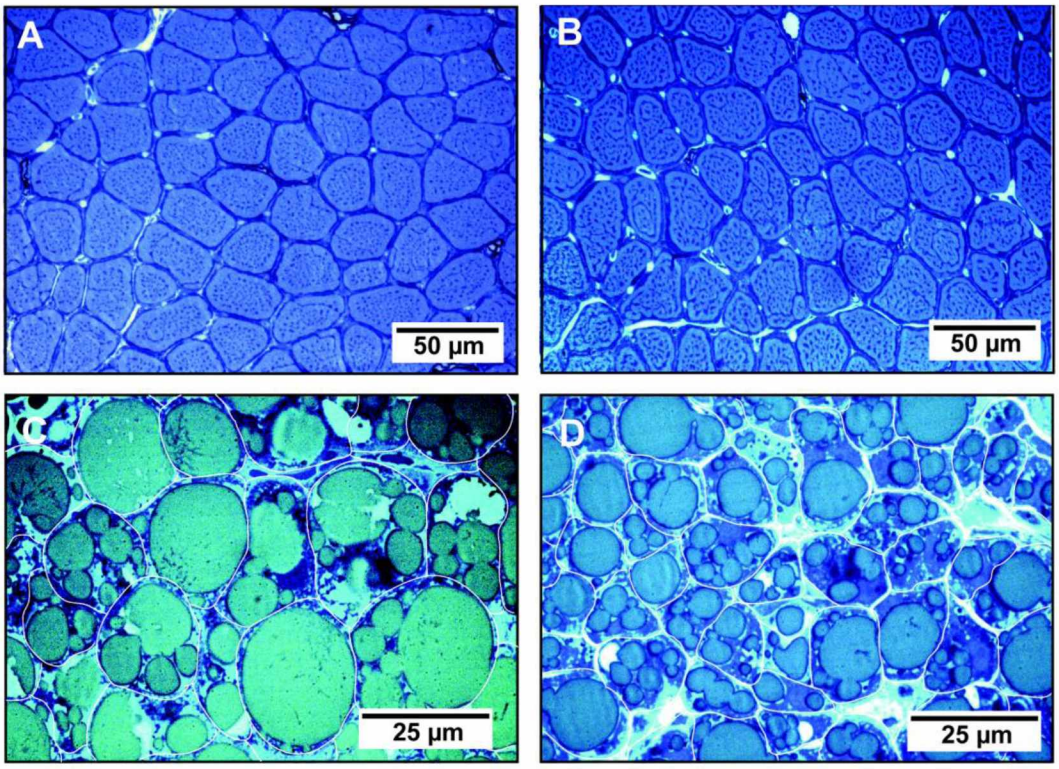

Fig. B.1. Light micrographs. Light micrographs of oxidative muscle fibers (A and B) and liver tissue (C and D) from warm- (A and C) and cold- (B and D) acclimated sticklebacks held at 20°C for 9 weeks and 8°C for 9 weeks.

Table B.1 Subsarcolemmal and intramyofibrillar mitochondrial densities

	20°C wk 9	8°C wk 9
Vv(ss mit,f) (%)	12.47 ± 1.75	23.74 ± 1.84*
Vv(imf mit,f) (%)	1.02 ± 0.17	1.65 ± 0.11*

Values are presented as means ±SE, (N=4). *Vv*, volume density; f, fiber; imf, intramyofibrillar; mit, mitochondria; ss, subsarcolemmal. *Significantly different between warm- and cold-acclimated fishes within a tissue ($P < 0.05$)

Table B.2 Total RNA mg tissue^{-1} during cold acclimation

Time point (N)	Liver	Oxidative Muscle	Glycolytic Muscle
20°C (12)	1.08±0.19	0.53±0.04‡	0.45±0.02‡
15°C (8)	0.55±0.19	0.42±0.04	0.39±0.02‡
10°C (10)	0.35±0.14	0.24±0.03*	0.28±0.03*
8°C (7-12)	0.87±0.16	0.18±0.04*	0.14±0.03*
1 week 8°C (8-12)	1.11±0.25	0.09±0.02‡*	0.24±0.05*
4 week 8°C (8)	1.67±0.22	0.25±0.10*	0.46±0.06‡
9 week 8°C (11)	1.79±0.33	0.73±0.08‡	0.85±0.08‡*
9 week 20°C (12)	0.87±0.15	0.32±0.04*	0.25±0.02*

Values are presented as mean ± SE. *Significantly different from animals at 20°C.
‡Significantly different from animals at 20°C wk 9.

Fig. B.2 18S rRNA cDNA sequence (ENSGACG00000021793). Boxed sequences indicate forward and reverse primers used for qRT-PCR.

Fig. B.3 Citrate synthase cDNA sequence (ENSGACG00000010851). Shaded diamonds denote predicted splice sites and boxed sequences indicate forward and reverse primers used for qRT-PCR.

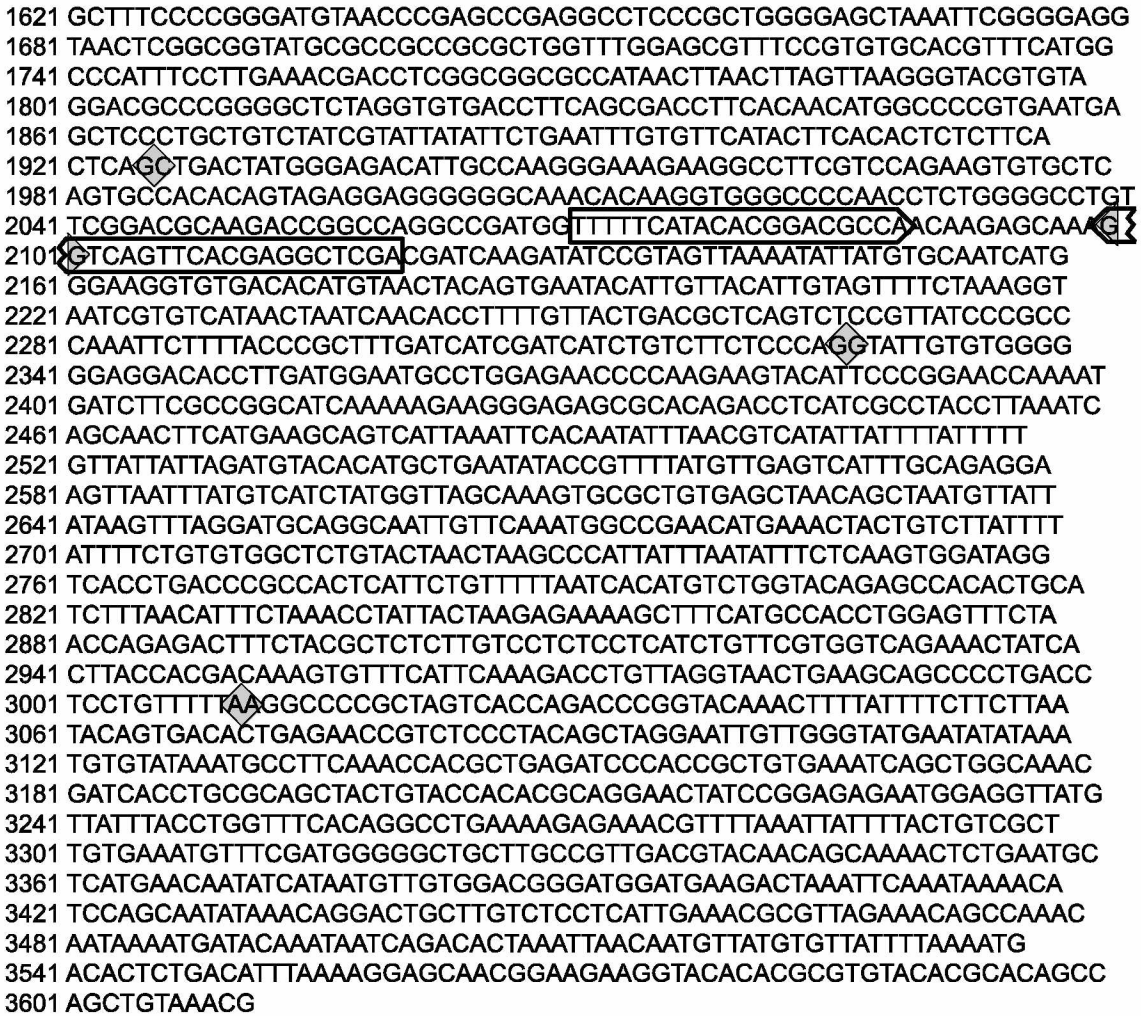

Fig. B.4 Partial cytochrome c cDNA sequence (ENSGACG00000011687). Shaded diamonds denote predicted splice sites and boxed sequences indicate forward and reverse primers used for qRT-PCR.

Fig. B.5 Cytochrome c oxidase cDNA sequences. Cytochrome c oxidase subunits III (ENSGACG00000020942) (A) and IV (ENSGACG00000015963) (B). Shaded diamonds denote predicted splice sites and boxed sequences indicate forward and reverse primers used for qRT-PCR.

Fig. B.6 Elongation Factor-1α cDNA sequence (ENSGACG00000002143). Shaded diamonds denote predicted splice sites and boxed sequences indicate forward and reverse primers used for qRT-PCR.

Fig. B.7 Mitochondrial Transcription Factor-1α cDNA sequence (ENSGACG000000 15427). Shaded diamonds denote predicted splice sites and boxed sequences indicate forward and reverse primers used for qRT-PCR.

Fig. B.8 Nuclear Respiratory Factor-1 cDNA sequence (ENSGACG00000019712). Shaded diamonds denote predicted splice sites and boxed sequences indicate forward and reverse primers used for qRT-PCR.

Fig. B.9 Peroxisome Proliferator-activated Receptor γ Coactivator-1 cDNA sequences. Peroxisome proliferator-activated receptor γ coactivator-1α (ENSGACG00000019546) (A) and β (ENSGACG00000016810) (B). Shaded diamonds denote predicted splice sites and boxed sequences indicate forward and reverse primers used for qRT-PCR.

Fig. B.10 TATA-Box Binding Protein cDNA sequence (ENSGACG00000016147). Shaded diamonds denote predicted splice sites and boxed sequences indicate forward and reverse primers used for qRT-PCR.

Fig. B.11 β-Actin cDNA sequence (ENSGACG00000007836). Shaded diamonds denote predicted splice sites and boxed sequences indicate forward and reverse primers used for qRT-PCR.